Contract Report CERC-93-1
August 1993

US Army Corps of Engineers
Waterways Experiment Station

Full Boltzmann Discrete Spectral Wave Model, Implementation and Nondimensional Tests

by Donald T. Resio
Florida Institute of Technology

Approved For Public Release; Distribution Is Unlimited

Prepared for Headquarters, U.S. Army Corps of Engineers

The contents of this report are not to be used for advertising, publication, or promotional purposes. Citation of trade names does not constitute an official endorsement or approval of the use of such commercial products.

PRINTED ON RECYCLED PAPER

Contract Report CERC-93-1
August 1993

Full Boltzmann Discrete Spectral Wave Model, Implementation and Nondimensional Tests

by Donald T. Resio

Department of Oceanography, Ocean Engineering,
and Environmental Science
Florida Institute of Technology
Melbourne, FL 32901

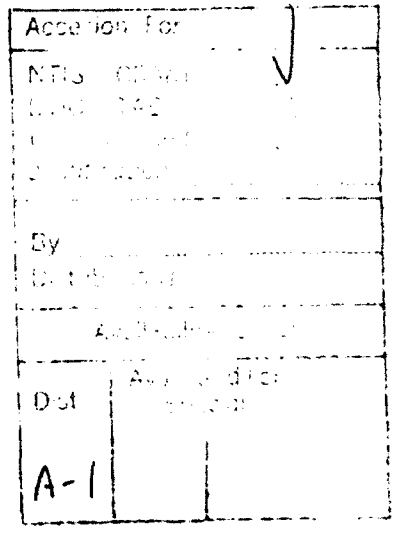

Final report

Approved for public release; distribution is unlimited

Prepared for U.S. Army Corps of Engineers

Under Work Unit 32523

Monitored by Coastal Engineering Research Center
U.S. Army Engineer Waterways Experiment Station
3909 Halls Ferry Road, Vicksburg, MS 39180-6199

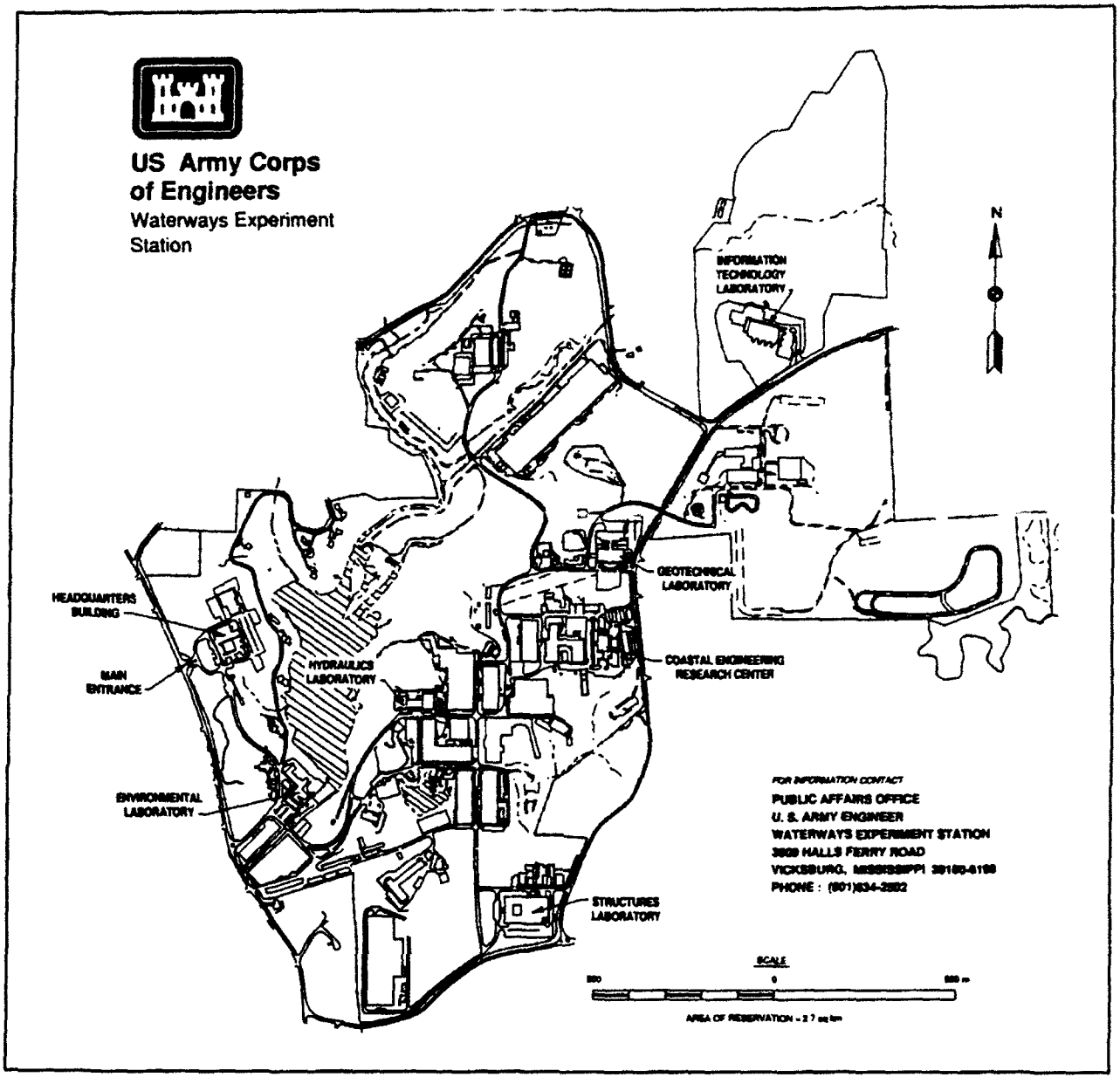

Waterways Experiment Station Cataloging-in-Publication Data

Resio, Donald T.

Full Boltzmann discrete spectral wave model, implementation and non-dimensional tests / by Donald T. Resio; prepared for Headquarters, U.S. Army Corps of Engineers.

51 p.: ill.; 28 cm. -- (Contract report; CERC-93-1)

Includes bibliographical references.

1. Ocean waves -- Mathematical models. 2. Spectrum analysis. 3. Water waves -- Mathematical models. 4. Transport theory. I. United States. Army. Corps of Engineers. II. Coastal Engineering Research Center (U.S.) III. U.S. Army Engineer Waterways Experiment Station. IV. Title. V. Series: Technical report (U.S. Army Engineer Waterways Experiment Station); CERC-93-1.

TA7 W34c no.CERC-93-1

Contents

Preface

This study was authorized by Headquarters, U.S. Army Corps of Engineers (HQUSACE) under Civil Works Research Work Unit 32523, "Upgrading of Discrete Spectral Hindcasting Models," Coastal Flooding Program. Messrs. John H. Lockhart, Jr., John G. Housley, Barry W. Holliday, and David A. Roellig were HQUSACE Technical Monitors. This report was prepared by Dr. Donald T. Resio, Florida Institute of Technology. The report was reviewed by Drs. Robert E. Jensen and C. Linwood Vincent, and Ms. Barbara A. Tracy, U.S. Army Engineer Waterways Experiment Station (WES) Coastal Engineering Research Center (CERC). Dr. Jensen's work was carried out under the program management of Dr. Vincent and Ms. Carolyn Holmes, CERC; under the direct supervision of Mr. H. Lee Butler, Chief, Research Division; and under the general supervision of Dr. James R. Houston and Mr. Charles C. Calhoun, Jr., Director and Assistant Director, CERC, respectively.

At the time of publication of this report, Director of WES was Dr. Robert W. Whalin. Commander was COL Bruce K. Howard, EN.

1 Introduction

Early wave prediction methods were based on nondimensional relationships among various wave generation parameters (Sverdrup and Munk 1947; Pierson, Neumann, and James 1955; Bretschneider 1952). These methods treated the entire wave spectrum as though it was equivalent to a single wave train, and the resulting models have been subsequently termed parametric wave models. By the early 1960's, a large body of evidence had accumulated which clearly demonstrated that waves in nature are better represented by a linearly superposed directional spectrum than by parametric wave trains. This motivated initial development of discrete spectral wave prediction models (Gelci, Cazale, and Vassal 1957). In this type of model, individual discretized components of a directional wave spectrum are modeled independently, except for parametric constraints on the local wave steepness as postulated by Phillips (1958).

Since the work of Hasselmann in the early 1960's (Hasselmann 1962, 1963a,b), a strong theoretical foundation for the estimation of nonlinear energy transfers in a gravity wave spectrum has existed. However, most researchers in the 1960's believed nonlinear interactions to be so weak that they were not significant to the overall wave generation process. Since no field evidence existed to contradict this belief and since numerical methods and computers were not available to evaluate the complete integral for nonlinear wave-wave interactions, the evolution of a wave spectrum was believed to be controlled only by direct wind input and wave breaking (Phillips 1957, Miles 1957, Bunting 1970). Under this assumption, the concept of an equilibrium range in a spectrum was formulated as an absolute limit to wave steepness, controlled only by wave breaking (Phillips 1958).

Following the theoretical concepts of Phillips (1957, 1958) and Miles (1957), early discrete-spectral wave prediction models were based on the concept that direct wind input was the primary mechanism in wave generation. In these models the equilibrium range related only to an absolute steepness (Inoue 1967, Bunting 1970, Cardone, Pierson, and Ward 1976). Models of this type have been termed first-generation wave models.

Evidence contradicting this direct-wind-input concept of wave generation began to appear in studies in the late 1960's (Mitsuyasu 1968a,b); and in 1973 data from the Joint North Sea Wave Project (JONSWAP) experiment, along

with a synthesis of several other data sets (Hasselmann et al. 1973), demonstrated that energy levels in the equilibrium range varied systematically as a function of wind speed and fetch. This evidence, along with observations of "overshoot/undershoot" in energy levels near the spectral peak (Barnett and Wilkinson 1967, Barnett and Sutherland 1968) indicated that nonlinear interactions among wave components played an important role in wave generation. Calculations of the form of net source terms for wave spectra propagating along a fetch (Mitsuyasu 1968a, Hasselmann et al. 1973) were also consistent with the idea that nonlinear effects (wave-wave interactions) were a dominant source term in the wave generation process.

Revised concepts of the physics governing wave generation (Barnett 1968, Mitsuyasu 1968b, Hasselmann et al. 1973) and the recognition of potential prediction problems inherent in first-generation models (Resio 1981, Resio and Vincent 1982) motivated the development of discrete-spectral models incorporating nonlinear wave-wave interactions as an active source term. Such models have been termed second-generation models. Early models of this type (Barnett 1968, Ewing 1971) still assumed that energy levels in the equilibrium range were controlled only by wave breaking, and that hence, an absolute limit to wave steepness existed in the equilibrium range. Models such as this were still characterized by spectral evolution through time and space similar to that of first-generation models. Later models, such as that of Resio (1981), recognized the importance of allowing energy levels in the equilibrium range to vary systematically as a function of certain wave generation parameters. Models of this class have been found to produce results that are consistent with observed patterns of temporal and spatial wave growth.

In second-generation models, the form of the wave spectrum is assumed to be governed by a dynamic balance between wind input into the equilibrium range and the nonlinear flux of energy out of this region of the spectrum via nonlinear wave-wave interactions. Hasselmann et al. (1976) argued that the strength of the shape-stabilizing effects inherent in this dynamic balance was so dominant in the spectral evolution equation that wave spectra in nature always stayed fairly close to a prescribed equilibrium form. In fact, Hasselmann et al. argued that the dominance of this dynamic balance was sufficient to allow the spectrum to be modeled by simple parametric methods comparable to those of Bretschneider (1952). Recently, however, Hasselmann and Hasselmann (1985), and Hasselman et al. (1985a,b) have introduced a class of wave models in which it is assumed that the shape-stabilizing effects of wave-wave interactions are not sufficiently dominant to control spectral shape. Such wave models are termed third-generation models. In these models constraints on energy levels in the spectrum (up to frequencies about twice that of the spectral peak) are removed and the spectrum is allowed to vary as a function of the actual estimated source terms. At frequencies above about twice the spectral peak frequency, a prescribed parametric tail is employed to maintain stability and computational efficiency.

Due to its significance in controlling both spectral shape and wave growth, the proper evaluation of the nonlinear source function is of central importance

to the implementation of a valid third-generation wave model and, consequently, is critical to understanding the physics of wave generation. For such reasons, Hasselmann et al. (1985a) investigated four different means of obtaining estimates of the nonlinear source term. As will be shown subsequently in this report, none of the four methods investigated in that earlier study has been shown to produce reliable (within a factor of 2 accuracy) estimates of the nonlinear source term over the entire spectrum for a wide range of spectral shapes.

Recent work by Perrie and Resio (1993) has shown that proper specification of all source terms is critical to the accurate simulation of wave growth in wave models that attempt to use the principle of detailed balance in their predictive equations (i.e., all third-generation wave models). Of particular significance in the Perrie and Resio results is the determination of a critical frequency f_c, which represents a point of zero net flux in the nonlinear energy fluxes. For a JONSWAP spectrum with a peakedness parameter equal to 3.3, this frequency is equal to 1.50 times the frequency of the spectral peak. Since there are no net nonlinear energy transfers across this frequency, all energy entering the spectrum at lower frequencies is retained as net wave growth. Consequently, it is clear that the accurate specification of f_c is absolutely critical to predictions of total wave growth. If a nonlinear source term is poorly specified, it cannot be expected to accurately determine the location of f_c in arbitrary spectra.

The purpose of the effort described in this report is to revisit the problem of specifying the nonlinear source term and to incorporate a more accurate form for representing these interactions into a functioning wave model. For this purpose, rather than to attempt additional parameterizations, we use a full Boltzmann integral of the Resio-Perrie (1991) type. For the first time ever, this will enable us to obtain very accurate estimates of the nonlinear source term. This, in turn, should allow us to address some important questions relating to spectral evolution under turning winds, swell decay, and the approach to fully developed form. In a sense, the full Boltzmann model (FBM) represents the first third-generation model with a truly accurate representation of the nonlinear source term. However, it should be recognized that this model is very "young." In its present state of development, it is a functioning research-mode model; but it should in no way be regarded as an operational wave model. The only other existing third-generation wave model, the WAM model (from the acronym WAve Model), was under development by a staff of several scientists and engineers for over five years before it was made into an operational model; and, six years later, it still is being modified in its operational mode.

As a second part of this study, the authors will apply the FBM to the Surface Wave Dynamics Experiment (SWADE) results. This will provide insight into the detailed balance of mechanisms responsible for the observed wave growth and decay in some relatively complex situations. The SWADE wind fields and measured data have not yet been released for the second part of this study, so those comparisons will be reported in a separate report.

2 Previous Representations of Nonlinear Energy Transfers in a Wave Spectrum

Representations of the Complete Interaction Integral

Hasselmann's (1962) representation of the rate of change of energy density at a given location within a wave spectrum involves four interacting waves and is of the form (Hasselmann and Hasselmann 1981)

$$n(\underline{k}) = \int_0^\infty\int_0^\infty\int_0^\infty\int_0^\infty\int_0^\infty\int_0^\infty C(\underline{k}_1,\underline{k}_2,\underline{k}_3,\underline{k}_4)\ \delta(\underline{k}_1+\underline{k}_2-\underline{k}_3-\underline{k}_4)\delta(\omega_1+\omega_2-\omega_3-\omega_4) \tag{1}$$

$$n(k_1)n(k_3)[n(k_4)-n(k_2)]\ +n(k_2)n(k_4)[n(k_3)-n(k_1)]d\underline{k}_2 d\underline{k}_3 d\underline{k}_4$$

where

$\underline{k}_i$ = wave number vector specifying the location of the i^{th} interacting wave within the spectrum

ω_i = radial frequency of the i^{th} interacting wave

$n(k_i)$ = action density of the i^{th} interacting wave, $C(.)$ is the coupling coefficient which describes the strength of the interactions

$\delta(.)$ = Dirac delta function

It should be noted that the form of Equation 1 ensures conservation of action, energy, and momentum. Webb (1978) provided a transformed version of Equation 1 as

$$\frac{\partial n(\underline{k}_1)}{\partial t} = 2\int_0^\infty\int_0^\infty T(\underline{k}_1,\underline{k}_3)d\underline{k}_3 \tag{2}$$

where

$T(\underline{k}_1,\underline{k}_3)$ = transfer of action from $\underline{k}_3$ to $\underline{k}_1$, given by

$$T(\underline{k}_1,\underline{k}_3) = \oint C(\underline{k}_1,\underline{k}_2,\underline{k}_3,\underline{k}_4)D(\underline{k}_1,\underline{k}_2,\underline{k}_3,\underline{k}_4)\left|\frac{\partial W}{\partial n}\right| H(\underline{k}_1,\underline{k}_3,\underline{k}_4)\, ds \tag{3}$$

where

$$D(\underline{k}_1,\underline{k}_2,\underline{k}_3,\underline{k}_4) = n(\underline{k}_1)n(\underline{k}_3)[n(\underline{k}_4)-n(\underline{k}_2)] + n(\underline{k}_2)n(\underline{k}_4)[n(\underline{k}_3)-n(\underline{k}_1)]$$

In Equations 2 and 3 the interactions are now prescribed along an interaction locus, with s and n representing unit vectors along and across the locus, respectively, and $W=\omega_1+\omega_2-\omega_3-\omega_4$. The function $H(\underline{k}_1,\underline{k}_3,\underline{k}_4)$ is defined as

$$H(\underline{k}_1,\underline{k}_3,\underline{k}_4) = 1 \quad \text{when} \quad |\underline{k}_1-\underline{k}_3| \le |\underline{k}_1-\underline{k}_4|$$

$$= 0 \quad \text{when} \quad |\underline{k}_1-\underline{k}_3| > |\underline{k}_1-\underline{k}_4|$$

Webb, Tracy, and Resio (1982), and Resio and Perrie (1991) have all shown that Equations 2 and 3 provide a stable form for evaluating nonlinear energy transfers within a spectrum. Hence, the numerical method described in Resio and Perrie (1991), based on this equation, will be used here in comparisons of given approximations to the full Boltzmann integral.

An advantage to the form of Equations 2 and 3 over Equation 1 is inherent in the reduction of the integration over $\underline{k}_2$ and $\underline{k}_4$ to contributions along a specific interaction locus for each given combination of $\underline{k}_1$ and $\underline{k}_3$. In a numerical approximation of Equation 3, $\underline{k}_1$ and $\underline{k}_3$ can be specified precisely as the centers of integration grid cells (Figure 1). The values of $\underline{k}_2$ and $\underline{k}_4$ are then fixed to fall along appropriate interaction loci. The error in the evaluation of the location of $\underline{k}_2$ and $\underline{k}_4$ (and the action densities at these locations) is limited only by the accuracy of the numerical solution of the locus equation. This can be specified independent of the size of the integration grid cells.

In integration methods based on Equation 1, interacting sets of wave numbers are specified to an accuracy limited by the discretized accuracy of the integration grid. As pointed out previously, any two of the wave numbers can be arbitrarily specified to coincide with points in the discretized integration

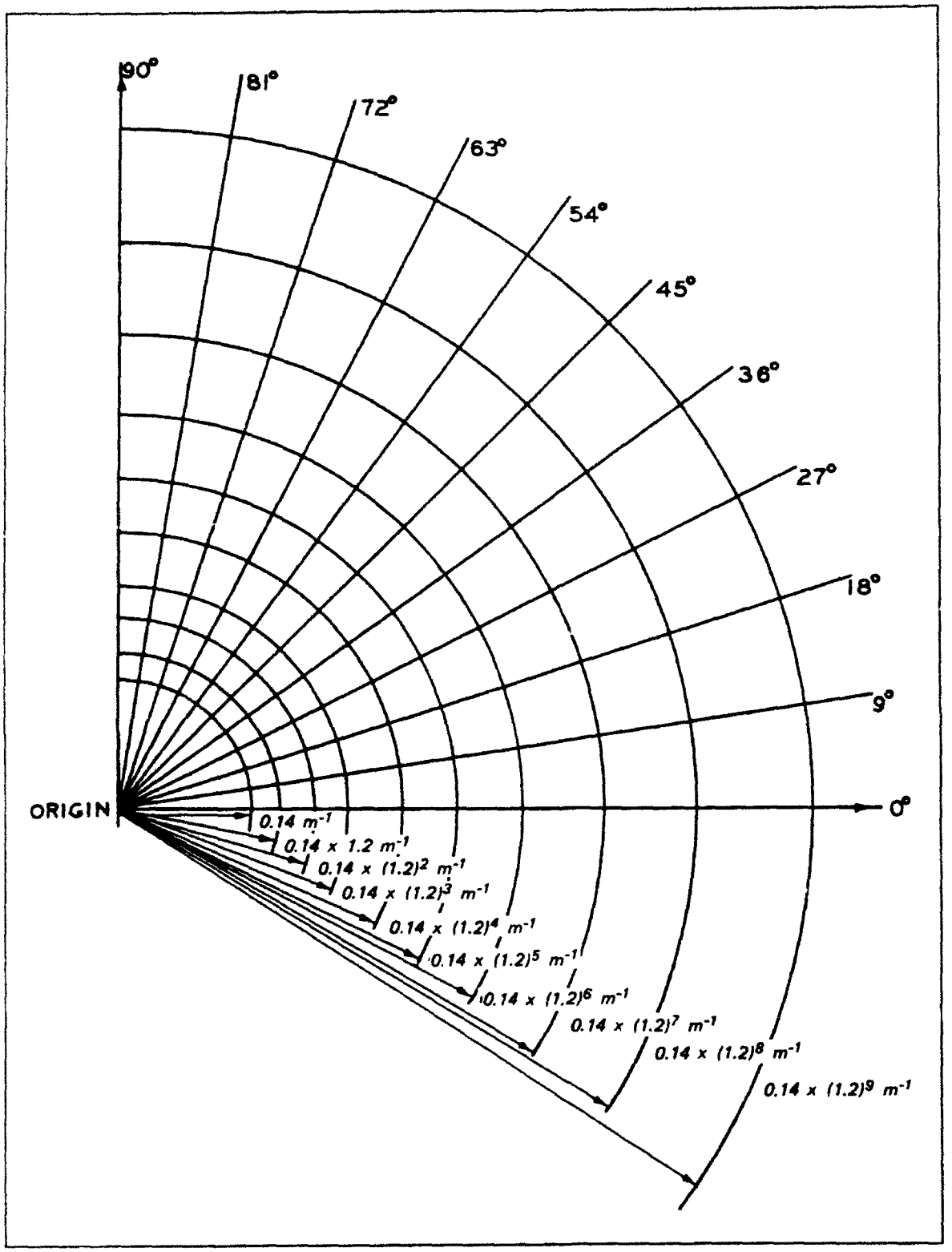

Figure 1. Specification of integration grid. Each point exactly coincides with $\underset{\sim}{k}_1$ and $\underset{\sim}{k}_3$ points in the integration space (Tracy and Resio 1978)

grid, with no loss of generality. The other two wave numbers are also approximated by values at the center of their grid cells. Although the delta functions are formally removed from the integral, the value for the energy density is taken from the discretized location of the center of the integration grid cell. This allows an exploitation of certain symmetries in the interaction integral (Hasselmann and Hasselmann 1981). However, as shown in Figure 2, if $\underline{k}_1$ and $\underline{k}_3$ are chosen to be coincident with fixed grid points, then the loci of points satisfying the wave number delta-function constraint will in general not be coincident with grid points. Thus, the assumptions that the six-fold collision integral can be written as a symmetric eight-fold integral will lead to inaccuracies in locations of the wave number positions used in the calculations. In turn, this produces quasi-random deviations around the correct integral solution for the nonlinear transfer source function S_{nl} as was shown by Resio and Perrie (1991) in a comparison of calculation of the Hasselmann and Hasselmann (1981) results to those based on an integral directly along the locus.

Representations of Parameterizations of the Interaction Integral

To date, methods for estimating the nonlinear source term due to wave-wave interactions in wave spectra can be divided into four main categories:

a. Direct parameterizations based on spectral energy content and shape.

b. Parameterizations based on empirical orthogonal functions.

c. Parameterizations based on local interaction approximations.

d. Parameterizations based on selected integration domains of the total integral.

Each of these methods will be discussed in turn here. Also, the basic form of each will be presented, along with limitations in their accuracies and efficiencies.

Direct parameterizations

Barnett (1968) and Ewing (1971) both developed parameterizations of the nonlinear source term which depend explicitly on (a) total wave energy, (b) prescribed shape functions, and (c) scaling frequencies related to the location of the mean frequency. In this form the representation for the nonlinear source term S_{nl} is given by

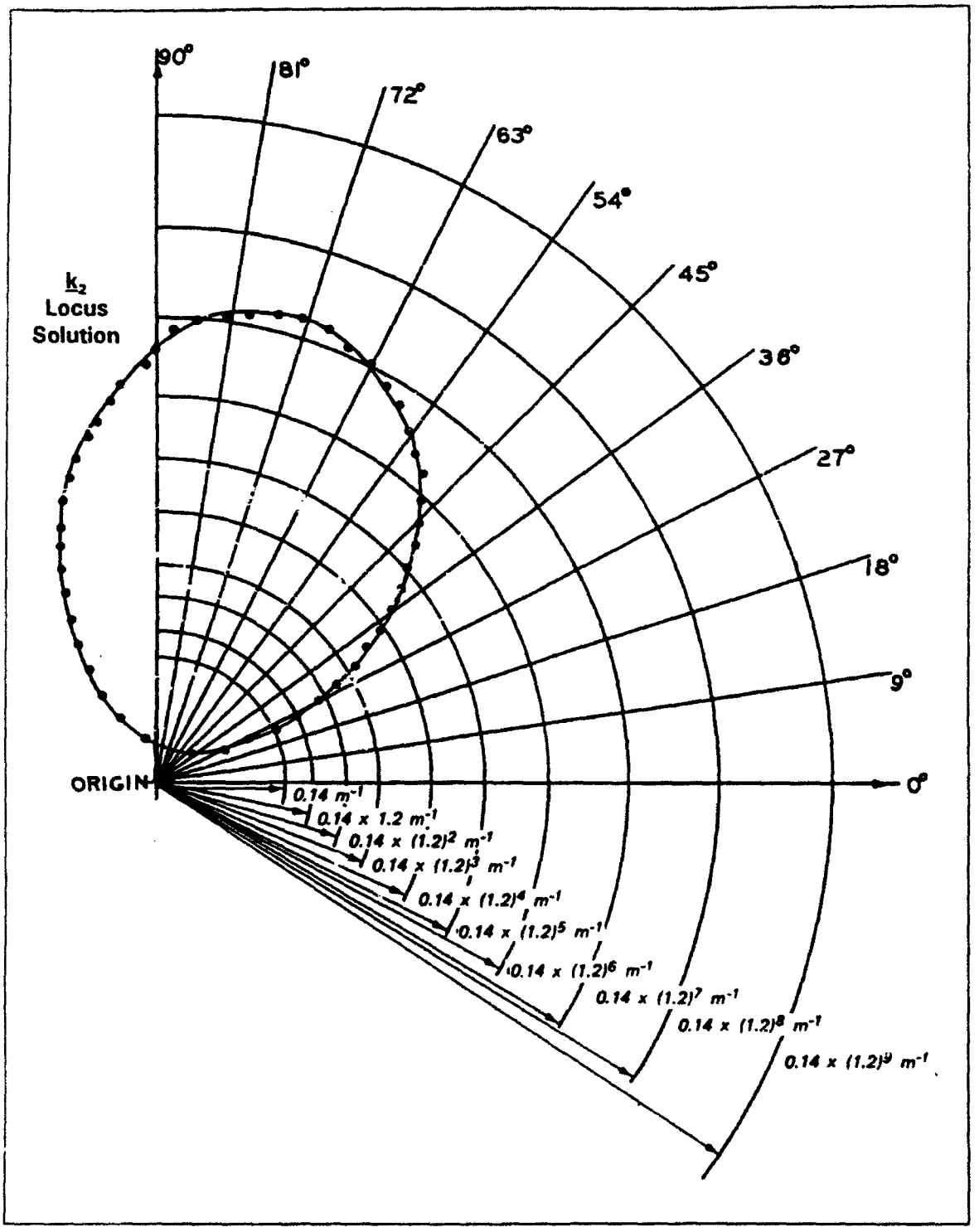

Figure 2. Comparison of locus solution for a fixed $\underline{k}_1$-$\underline{k}_3$ combination to the grid of integration points. The fixed integration points do not coincide with $\underline{k}_2$-$\underline{k}_4$ points; therefore, the two sets of points cannot be treated symmetrically

$$S_{nl} = \frac{\partial E(f,\theta)}{\partial t} = \phi_1(f_0,\theta_0)\phi_2(f/f_p)\phi_3(\theta-\theta_0) \tag{4}$$

where

θ_0 = mean wave propagation angle

E_0 = total energy in the wave spectrum, given by

$$E_0 = \int_0^{\infty}\int_0^{2\pi} E(f,\theta)\,df\,d\theta \tag{5}$$

where

$E(f,\theta)$ = spectral energy density at frequency f and propagation direction θ

f_o = a frequency scaling function of the form

$$f_0 = \left[\frac{1}{E_0}\int_0^{\infty} E(f) f^m\,df\right]^{\frac{1}{m}} \tag{6}$$

where

$E(f)$ = nondirectional spectral density, given by

$$E(f) = \int_0^{2\pi} E(f,\theta)\,d\theta \tag{7}$$

and m = a positive integer (usually taken to be equal to 1 or 2).

Resio (1981) recognized certain exact similarity characteristics of Equations 2 and 3 and chose to base his parameterization of S_{nl} by the form

$$S_{nl}(f,\theta) = \lambda\alpha^3 f_p^{-4}\phi_4(f/f_p)\phi_5(\theta-\theta_0) \tag{8}$$

where

α = equilibrium range coefficient for an f^{-5} equilibrium range

f_p = frequency of the spectral peak

ϕ_4, ϕ_5 = prescribed shape functions for frequency and angular characteristics, respectively

Since, at that time, it was widely believed that the spectral equilibrium range did follow an f^{-5} law (Phillips 1958, Kitaigorodskii 1961) and that spectral evolution along a fetch and through time followed a self-similar form (Mitsuyasu 1968b, Hasselmann et al. 1973, Toba 1978), this parameterization appeared to provide a reasonable approximation to the wave-wave interaction source term for spectra undergoing active wave generation (Figure 3).

Unfortunately, all of the parameterizations of this class are appropriate only for a narrow class of spectral shapes (albeit spectral shapes prevalent during most active wave generation scenarios). All of these parameterizations were formulated with the understanding that side conditions (such as the allowable energy levels in the equilibrium range) must be invoked whenever these parameterizations are used in predictive schemes. Hence, none of these parameterizations can be considered either sufficiently general or sufficiently unencumbered with constraints to be incorporated into a third-generation wave model.

Empirical orthogonal function (EOF) representations

The theoretical basis for EOF analyses shows that, for a given set of correlated variables (such as energy densities or S_{nl} at adjacent frequencies), an EOF analysis provides an optimal basis for representing a data set. Optimality in this context is taken as having the maximum variance explained in the smallest number of dimensions. Vincent and Resio (1977) showed that such an analysis for measured spectra at a site was capable of giving a good and efficient representation of nondirectional wave spectra in the absence of swell. However, in order to derive these functions one would have to have an *a priori* set of all possible spectra or S_{nl}'s (or at least a very large set) in order to form the covariance matrix for the EOF (eigenfunction) analysis. Such an analysis would be extremely difficult if, in fact, at all possible.

Hasselmann et al. (1985a) formulated a set of EOF's for a synthetic set of simulated spectra based on combinations of different nondirectional spectral shape parameters and angular spreading characteristics. Since an empirical parameterization can be no better than the data set on which it is based, it does not seem that much is gained by using the EOF's. A direct parameterization based on the spectral shape and angular spreading parameters themselves

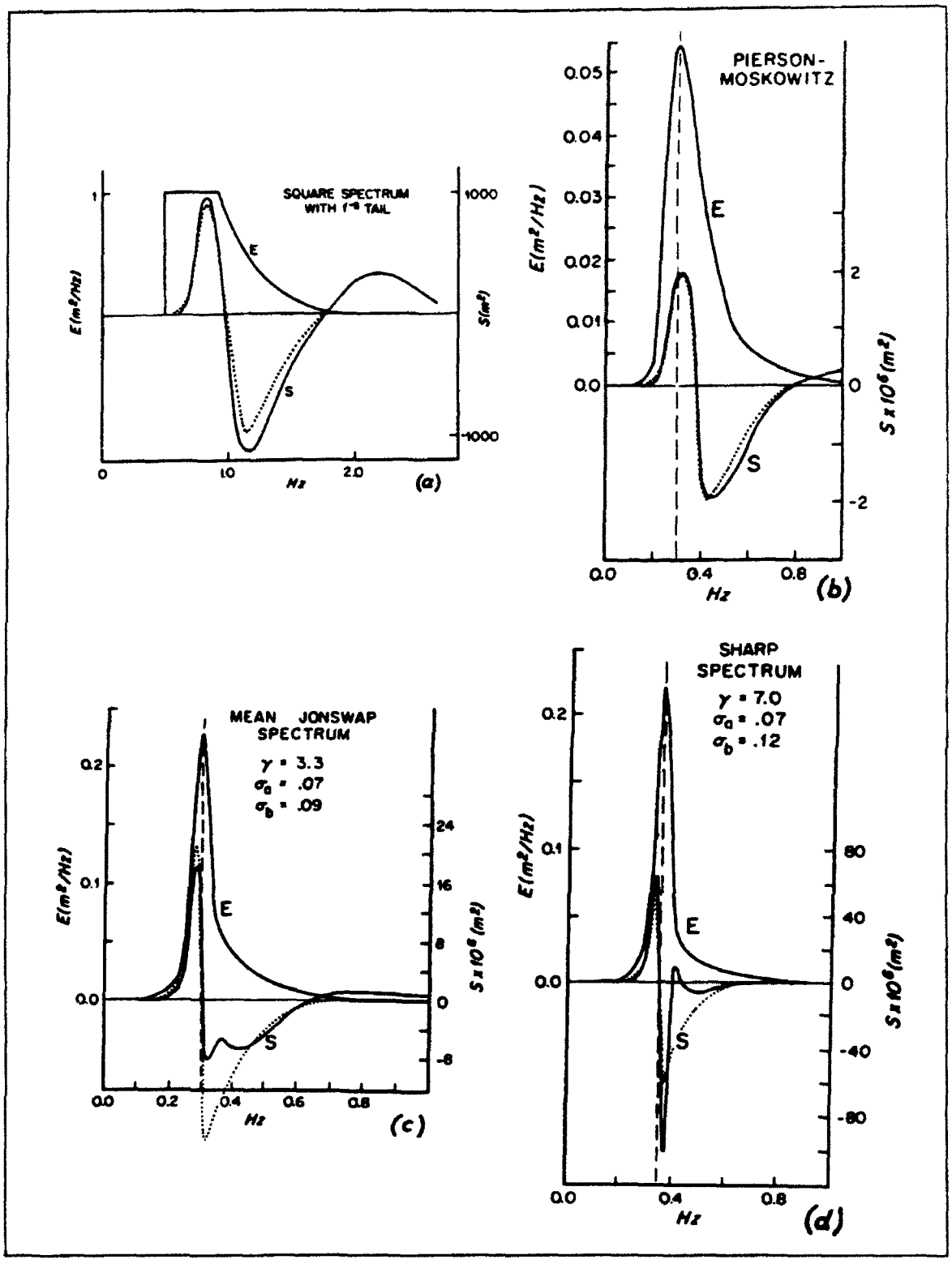

Figure 3. Parameterized nonlinear source terms compared to solution from full Boltzmann equation (Resio 1981)

appears to be more feasible. This approach offers interesting possibilities; but until the problem of a limited data set for analysis is overcome, it does not seem to be very practical.

Local interaction approximation

If one takes the full interaction integral and assumes that contributions to this integral are dominated by interactions that are close to $\underline{k}_1$ (using the notation consistent with Equations 2 and 3), then a local expansion can be used to develop a diffusion operator for representing S_{nl} (Hasselmann and Hasselmann 1981, Hasselmann et al. 1985a). This parameterization provides a better representation of S_{nl} as the spectral peakedness increases, since contributions to the total collision integral will be more restricted as this happens. Webb (1978) showed that significant contributions to S_{nl} at a given wave number can come from wave numbers quite removed from that wave number. Although this approximation does conserve action, energy, and momentum and does seem to follow the general shape of the actual form for S_{nl}, it cannot be considered as a general solution to the parameterization problem.

Discrete interaction approximation (DIA)

A final parameterization effort from Hasselmann et al. (1985a) is based on the representation of the total integral by an integral over a smaller subsection of the interaction space. This approximation assumes that the dominant interactions come from a small pre-defined region in wave number space. Details can be found in Hasselmann et al. (1985a) and will not be repeated here.

Figure 4 shows a comparison of the DIA parameterization of S_{nl} to the complete interaction integral for a JONSWAP spectrum from Hasselmann et al. (1985a). Agreement is quite poor in the equilibrium range of the spectrum. Since a third-generation wave model's purpose is to use the principle of detailed balance throughout the spectrum (up to at least 2.5 f_p or so), misrepresentations of S_{nl} in the equilibrium range can pose a serious problem. Due to the fact that the DIA is used in a third-generation wave model (WAMDIG 1988) that is widely distributed, it seems that additional comparisons are merited. Figure 5 shows a series of independent comparisons between the DIA and the total integral (Resio and Perrie 1993). The top two cases are spectra with directional shear in them. The bottom case is a typical swell spectrum with no shear. As can be seen there, the results suggest that the DIA provides only a rough approximation to the total integral for some spectra, and does not seem to provide an accurate, generalized representation for S_{nl}.

It would appear that at least a brief investigation into the reasons for DIA's failure in some of the cases shown in Figures 4 and 5 is in order. Perhaps the best way to view this is by examining what controls the strength of interacting waves (i.e., the rate of energy transfer from one part of the spectrum to another). Results of Webb (1978) demonstrate that energy transfers in and out

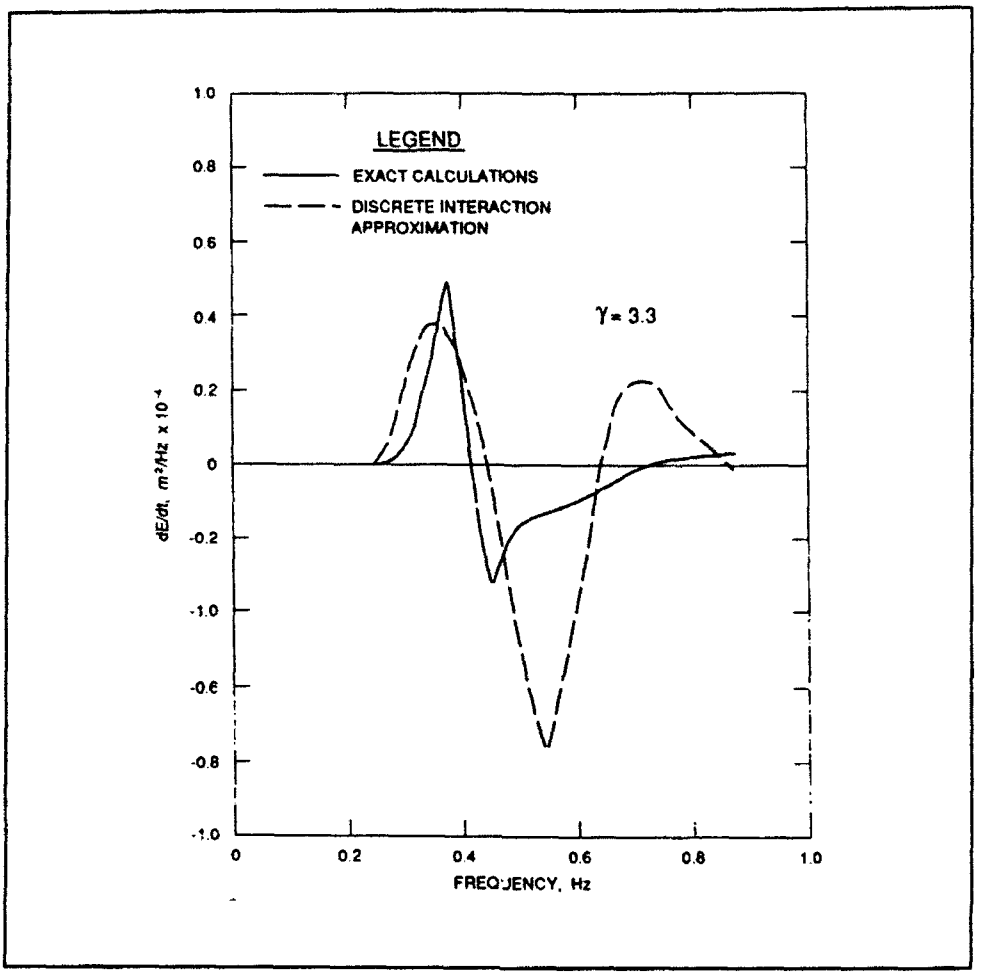

Figure 4. Comparison of DIA to complete Boltzmann integral (from Hasselmann et al. 1985a)

of a particular wave number location come from a rather broad region of wave number space and are not localized along preferred interaction locations. The reason for this broadness is straightforward. Contributions to the full integral can be separated into two different effects. The first effect depends on all of the "phase-space" effects, such as the coupling coefficient, the phase volume involved in the interaction, and the magnitude of the Jacobian term ($\partial W/\partial n$) in Equation 3. The second effect comes from the relative magnitudes of the action density triplets for each interaction volume. The first effect can be roughly parameterized in an *a priori* sense (which is the basis for the DIA). This assumes all interactions outside of the relatively small DIA region are negligible. The latter effect depends on details of the specific wave spectrum and cannot be parameterized via an *a priori* limitation to the integration region. Hence, the DIA cannot be accepted as a generalized representation for S_{nl}.

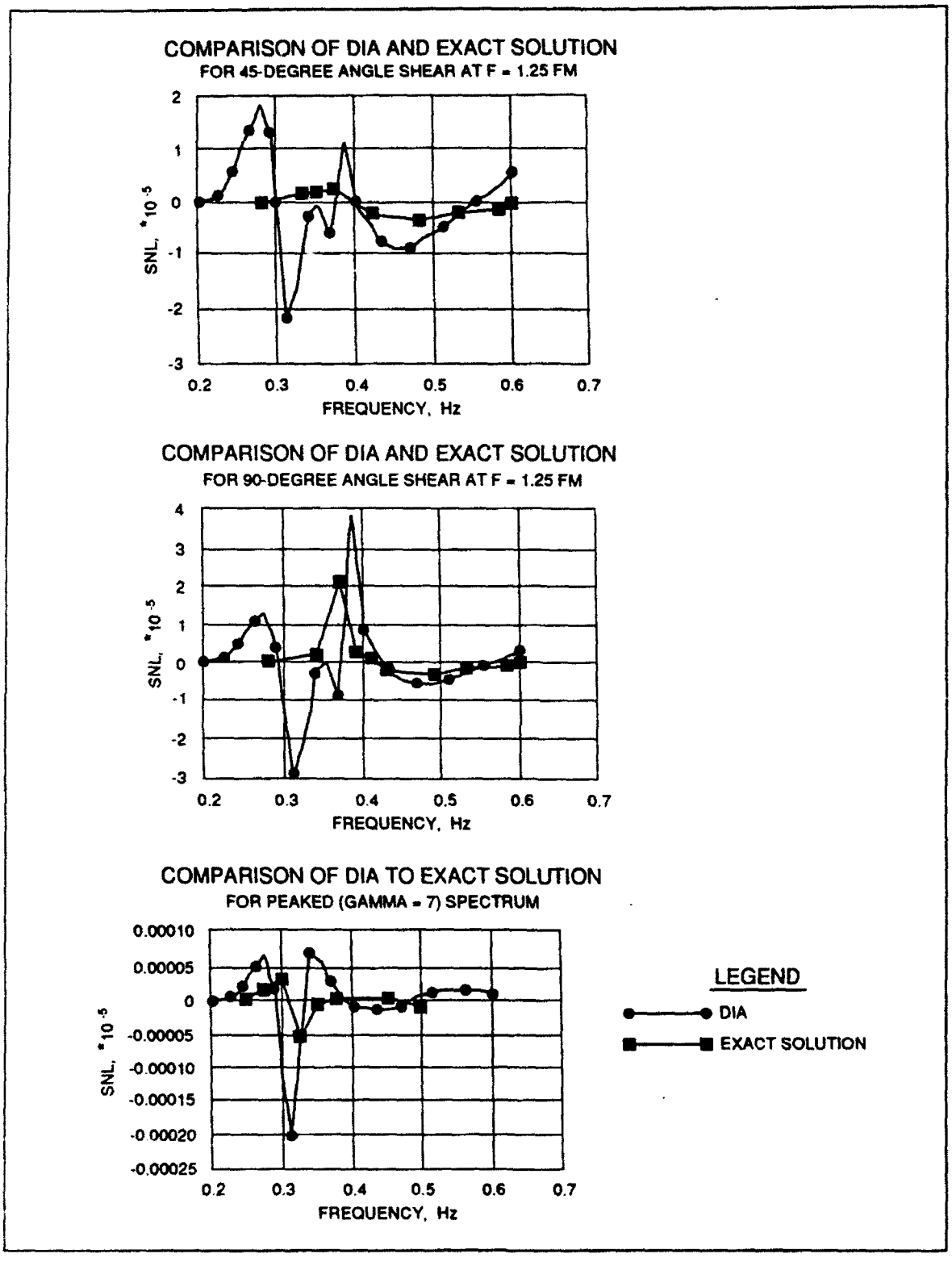

Figure 5. Comparisons of DIA to complete Boltzmann integral for turning wind situations

3 Implementation of a Full Boltzmann Representation for S_{nl} in a Discrete Spectral Wave Model

Although work on simplified representations for S_{nl} continues in various research groups around the world, no simplified method presently exists with an ability to accurately approximate the full Boltzmann solution. Due to the central importance of this source term in the wave generation process, development of third-generation wave models has been seriously hampered. In this class of wave models, parametric constraints placed on spectral shape in second-generation models are removed, and the spectrum is allowed to attain local equilibrium levels as dictated by the detailed balance of various source terms. Accurate source term representations are critical to the proper performance of such models.

The objective of this investigation has been to develop a discrete-spectral wave model that incorporates a complete representation of the Boltzmann integral for its wave-wave interaction source term. Even given today's powerful supercomputers, it is likely that this code will be useful only for research applications, rather than for climatological or forecast applications. However, this may change as faster computers and more efficient codes are developed in the future and as more experimentation is conducted with this type of model. In this section, the general structure of the prototype for this new model class, the FBM, will be discussed.

As shown in Figure 6, the overall structure of FBM follows along the same lines as the U.S. Army Engineer Coastal Engineering Research Center WISWAVE model (Hubertz 1992), with some simplifications where deemed appropriate. In particular, FBM is strictly a deep-water model, since no efficient numerical scheme presently exists for solving the full shallow-water Boltzmann integral.

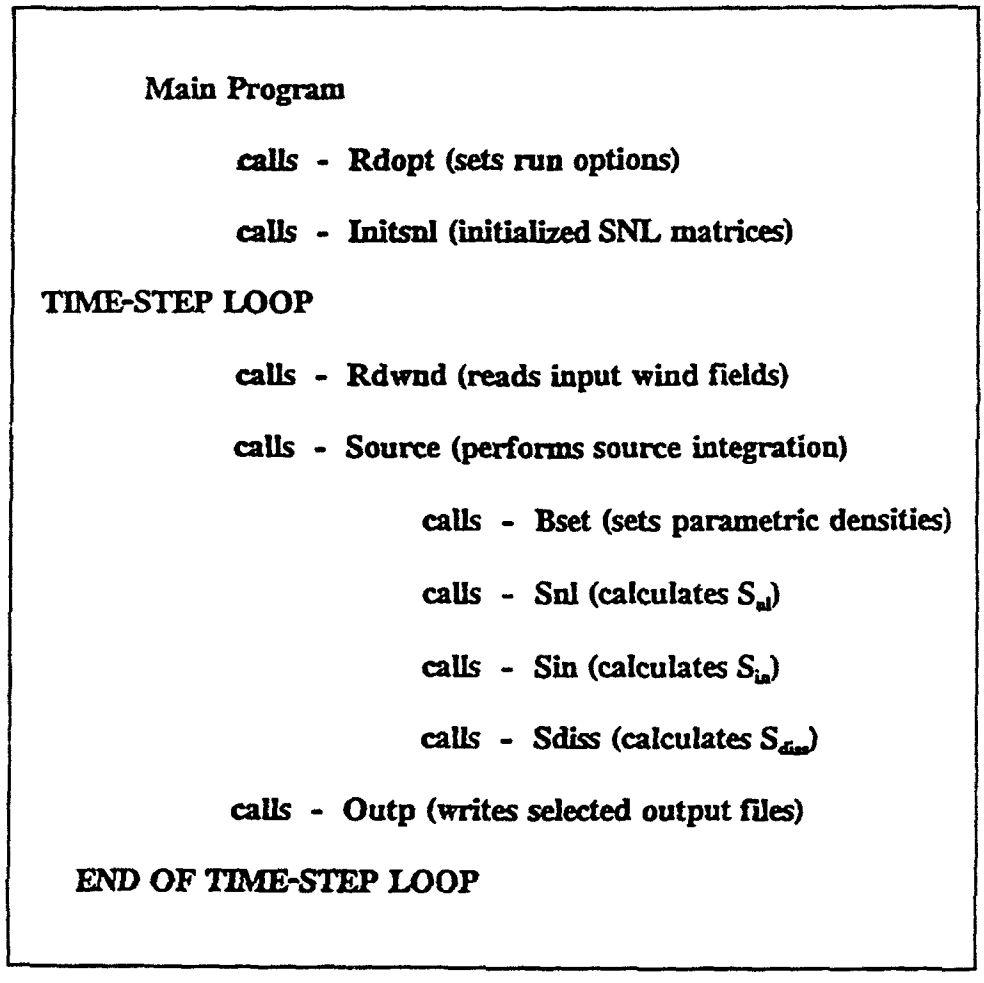

Figure 6. Outline of the structure of FBM

A discrete spectral wave model attempts to solve the general radiative transfer equation for each frequency-direction component of a spectrum. This equation has the general form

$$\frac{\partial E(f,\theta)}{\partial t} = \vec{c}_g \nabla E(f,\theta) + \sum_{k=1}^{3} S_k \qquad (9)$$

The first term of the right-hand side of Equation 9 represents the effects of wave propagation. The second term represents the effects of source and sink terms affecting spectral energy levels. This equation is an inhomogeneous partial differential equation. The solution technique solves the homogeneous part (propagation) first and the inhomogeneous part (source integration) second.

Under the present understanding of the physics of wave generation, it is believed that three source terms (wind input, nonlinear wave-wave interactions, and wave breaking (including high-frequency dissipation)) constitute the primary processes affecting deep-water wave growth and decay. The FBM is written in a modular fashion so investigators can modify and/or replace source functions as desired.

The most difficult aspects of implementing a full Boltzmann solution for S_{nl} into a wave model center around two problems. First, the full-integral solution is extremely nonlinear and formally extends over a range of frequencies from 0 to ∞; consequently, it can be extremely unstable. Second, actual knowledge of the detailed balance of the wind input and wave breaking source functions is quite limited. Attempts to argue definitively for a particular theoretical form of these source functions should be regarded with skepticism. Although FBM has a potential to answer important questions relevant to rates of nonlinear energy fluxes through a spectrum, it cannot be expected to provide definitive estimates of S_{in}, the wind input, or S_{ds}, wave breaking.

For the sake of efficiency, the domain for the Boltzmann integral will be limited to a reasonable size in wave number space. A problem with limiting the integration domain to less than some "cutoff" wave number, k_c, is that the collision integral at k_c will include all interactions from frequencies less than or equal to k_c but none from higher frequencies. This totally distorts the energy fluxes through k_c and misrepresents estimates of S_{nl} at k_c. To overcome this difficulty, FBM separates the infinite domain into four parts, as shown in Figure 7. In region I, it is assumed that wave-wave interactions are negligible and can be ignored; thus, the boundary condition between regions I and II is a zero-flux constraint. Region II is intended to cover the wave number range of a typical discrete spectral wave model. In this region, FBM allows the user to select the number of frequencies (wave numbers) and directions in a manner consistent with WISWAVE. Region III includes the range of frequencies that are "significantly" involved in interactions with wave components in region II. Since the boundary condition between regions III and IV cannot be specified (without extending the integral to ∞), energy levels within region III must be set parametrically. Once this is done, the boundary condition on fluxes between regions II and III is automatically specified by the interaction integral, given that the integration limit on k_3 in Equation 2 is allowed to extend to the boundary of region IV. The logical limit on the k_1 domain in Equation 2 is up to the lower boundary of region III. It is assumed that contributions to S_{nl} from region IV are negligible.

Some wave models contain linear atmospheric input terms of the form originally proposed by Phillips (1957). These models can start from an initial condition of zero energy. However, wave models with significant linear wind input terms have been shown to produce spectral shapes which deviate dramatically from observed spectra in nature (Resio and Vincent 1982). Therefore, FBM does not incorporate such a source term and instead relies on a parametric model for wave growth in regions III and IV. The equations for wave

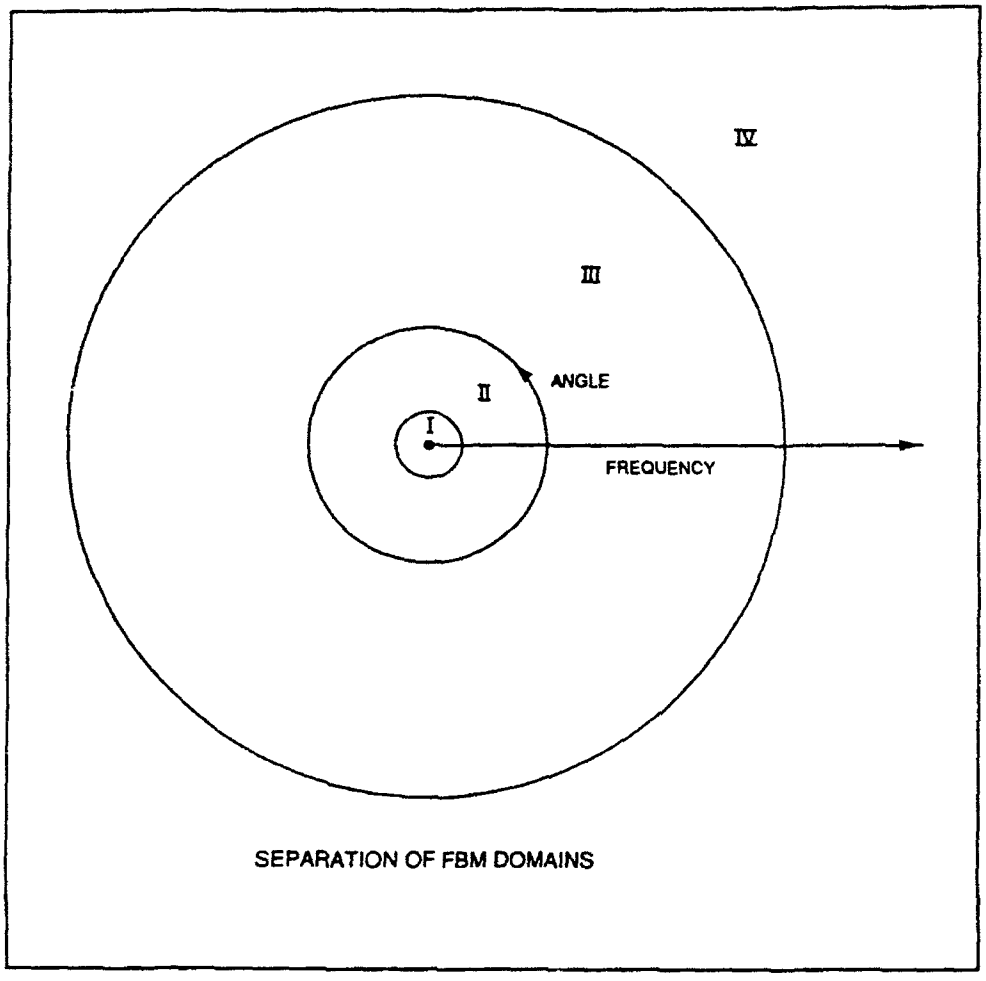

Figure 7. Separation of FBM domains

growth in these frequencies assume negligible propagation effects and follow the duration growth equations and spectral shape formulation given in Resio and Perrie (1989). These equations are used to calculate the frequency of the spectral peak f_p and associated spectral energy densities until f_p moves into region II of the simulation.

4 Source Term Development and Nondimensional Testing

In FBM, it is possible to vary (via simple internal switches in comments and executable statements) source functions in order to calibrate growth rates. The modular structure of FBM is such that all constants and functions inherent in S_{in} are set inside of subroutine SIN. Similarly, all constants and functions inherent in S_{ds} are set inside subroutine S_{ds}.

From considerations of spectral equilibrium range characteristics, approach to a fully developed spectrum, and net growth rates, the following source term balances are anticipated:

a. In the equilibrium range, divergence in the fluxes due to nonlinear interactions should be approximately balanced by the wind source term and wave breaking should be of secondary importance.

b. As a fully developed spectral form is approached, the wave breaking source term should approximately balance the positive source due to nonlinear fluxes of energy onto the forward face of a spectrum (at least in an integrated sense).

c. The rate of gain of total energy should be approximately self-similar; thus, due to the extreme shape-dependent behavior of the S_{nl}, the detailed balance of all source terms is expected to create evolving spectral shapes that maintain a reasonably consistent shape.

With the above guidance, literally hundreds of source-term combinations have been investigated inside FBM. In this section, we shall first examine the performance of FBM with wind input and wave breaking source terms from WAMDIG (1988). As will be seen here, these source terms do not produce wave growth rates or spectral shape characteristics that compare very well with observations. Because of the failure of the WAM source terms, FBM will also be tested with some new source terms.

The wind input source term referenced by WAMDIG (1988) follows the form of Snyder et al. (1981). Snyder et al.'s form is approximately given by

$$S_{in} = 0.25\frac{\rho_a}{\rho_w}\left[\frac{u_5\cos(\theta-\theta_w)}{c} - 1.\right]\omega E(f,\theta) \tag{10}$$

where

θ_w = direction of the wind

ρ_a = density of air

ρ_w = density of water

θ = wave propagation direction

ω = radial frequency

u_5 = wind speed at a level of 5 m

c = wave phase velocity

WAMDIG uses the following modified form of this equation, which is based on friction velocity u_* rather than wind speed.

$$S_{in} = 0.25\frac{\rho_a}{\rho_w}\left[28\frac{u_*}{c}\cos\theta - 1\right]\omega E(f,\theta) \tag{11}$$

The similarity to the previous equation is very evident. An unfortunate aspect of WAMDIG's form for S_{in} is that the limiting frequency for a fully developed sea has a dependence on friction velocity rather than wind speed. Previous studies (Pierson and Moskowitz 1964) have suggested that this limiting frequency be based on wind speed. No theoretical or empirical evidence has been presented which supports the use of u_* for scaling the limiting frequency in a fully developed sea.

The WAMDIG form for dissipation due to wave breaking has its theoretical basis in the work of Hasselmann (1974). Subsequently, Komen et al. (1984) "tuned" this term to provide a zero net source-term balance for a fully developed spectrum. The WAMDIG representation for S_{ds} is given by

$$S_{ds} = b\bar{\omega}\left(\frac{\omega}{\bar{\omega}}\right)^2\left(\frac{\alpha}{\alpha_{PM}}\right)^2 E(f,\theta) \tag{12}$$

where

b = empirical coefficient

α = equilibrium range coefficient

α_{PM} = Pierson-Moskowitz equilibrium range constant (0.0081), and

$$\overline{\omega} = \frac{1}{E_0} \int_{\sigma}^{\infty} \int_{0}^{2\pi} \omega E(f,\theta) df d\theta$$

where

$$E_0 = \int_{0}^{\infty} \int_{0}^{2\pi} E(f,\theta) df d\theta$$

Nondimensional Parameters for Testing

A substantial historical perspective exists (Bretschneider 1952, Mitsuyasu 1968, Hasselmann et al. 1973) for making wave comparisons in a nondimensional context. Hasselmann et al. (1973) added the extensive data set collected during JONSWAP to data from several previous studies and developed empirical laws governing relationships between pairs of nondimensional parameters, sometimes referred to as the JONSWAP relationships. These relationships will be used in this section to provide an observational context for all model predictions. The four relationships examined here will be nondimensional energy versus nondimensional fetch, nondimensional peak frequency versus nondimensional fetch, nondimensional energy versus nondimensional time, and nondimensional peak frequency versus nondimensional time. The definitions of these nondimensional parameters are as follows:

Nondimensional energy

$$E' = g^2 E_0 / u_*^4$$

Nondimensional fetch

$$x' = gx/u_*^2$$

where x is the fetch over which the wind blows.

Nondimensional peak frequency

$$f_p' = u_* f_p / g$$

where f_p is the spectral peak frequency, and

Nondimensional time

$$t' = gt/u_*$$

where t is the duration of the wind.

Testing with Existing Source Terms

Using the WAMDIG source terms with FBM produced the results for E' versus x', f'_p versus x', E' versus t', and f' versus t' shown in Figures 8-11. These results were obtained by running FBM with constant 10-m/sec and 20-m/sec wind speeds with the high-frequency tail constrained to an f^{-5} form.

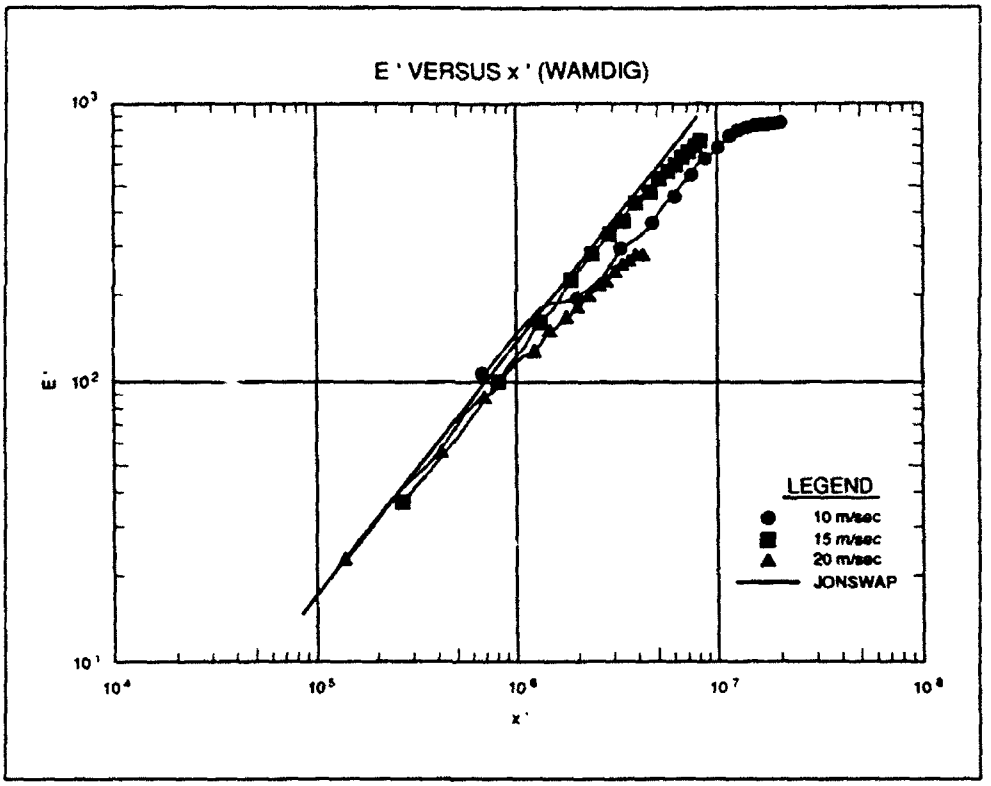

Figure 8. Comparison of FBM nondimensional energy growth rate with fetch (using WAMDIG (1988) source terms) to JONSWAP results

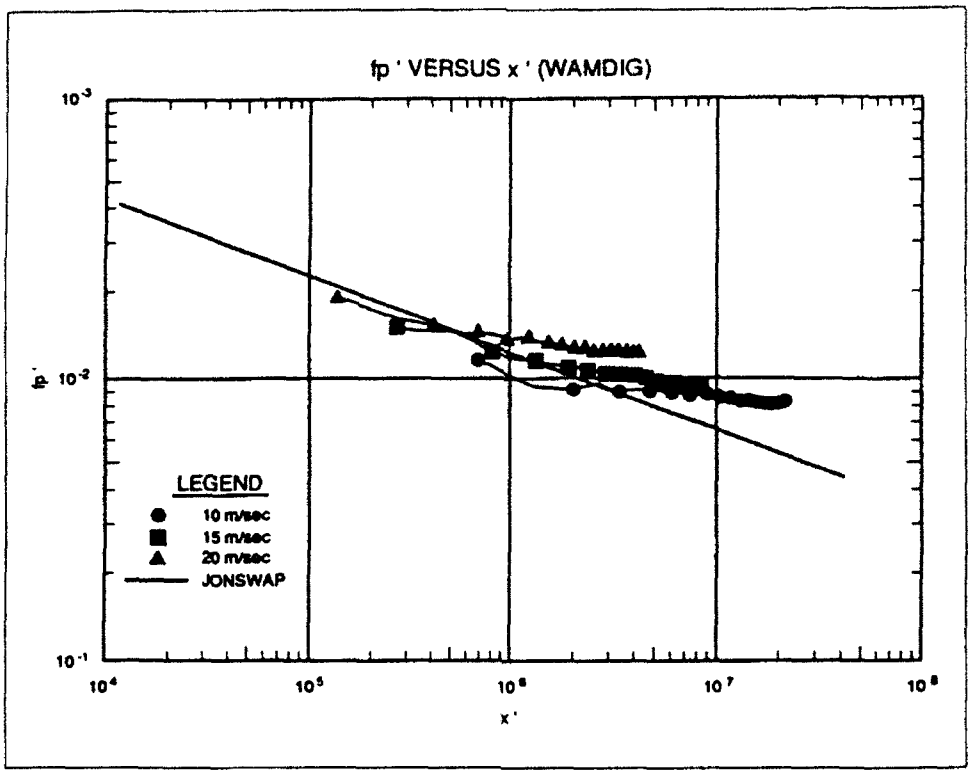

Figure 9. Comparison of FBM nondimensional peak frequency growth rate with fetch (using WAMDIG (1988) source terms) to JONSWAP results

Attempts to run using the WAM source terms with an unconstrained tail produced erratic results, so only results with the constrained tail are shown here. It should also be noted that portions of the WAMDIG results shown in these figures are produced by the parametric solution in region III of FBM. In the region governed by the detailed balance solution (region II), the WAMDIG results deviate dramatically from the JONSWAP relationships.

Fetch tests were conducted on an idealized basin with side boundary conditions equivalent to an infinitely wide fetch area. The length of the basin was 310 km with a grid size of 10 km. The time-step used in these simulations was 300 sec. The relatively short time-step was required to maintain stability in the evaluation of S_{nl}. Duration tests were conducted by setting the grid size very large (100,000 km) and using only a single grid point in the water portion of the grid. These tests were also run with a 300-sec time-step. The results of these tests are shown in Figures 10-11, along with the corresponding JONSWAP relationships. These results show that the source terms in WAMDIG (1988) do not reproduce the JONSWAP relationships. These tests also demonstrate that the treatment of the high-frequency tail significantly affects total wave growth. This latter finding is a direct contradiction of the discussion in Komen et al. (1984), which states that their wave growth results were not dependent on the characteristics of the high-frequency tail.

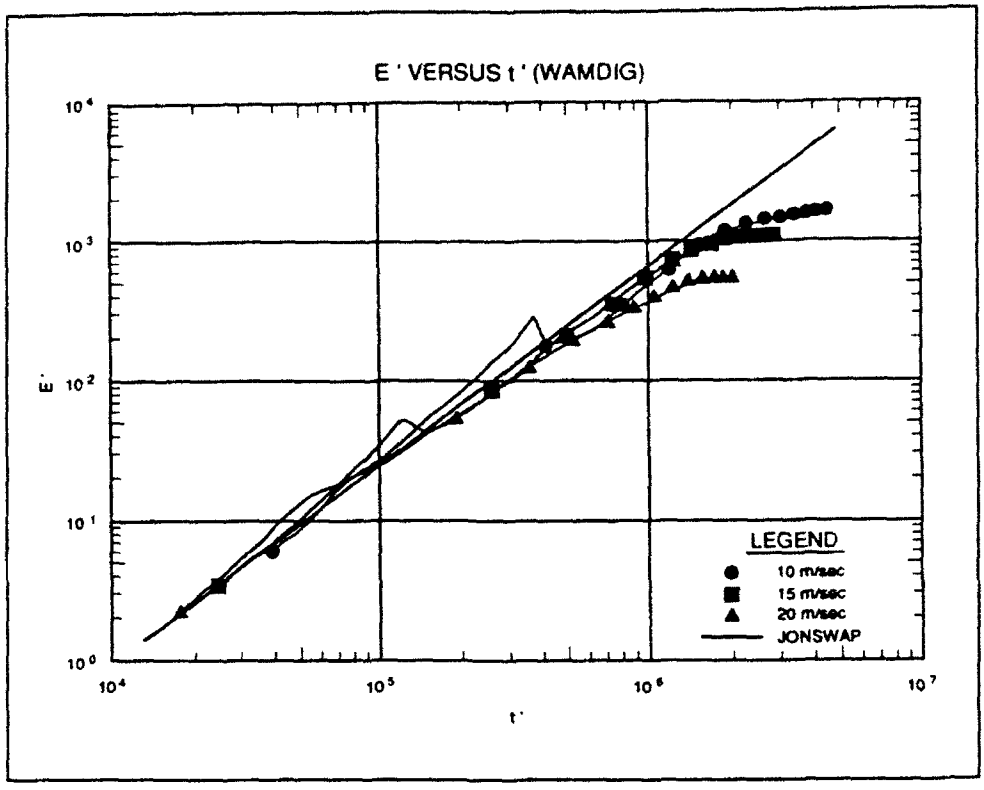

Figure 10. Comparison of FBM nondimensional energy growth rate with time (using WAMDIG (1988) source terms) to JONSWAP results

The above results were verified by running the WAMDIG source terms inside the Boltzmann integral of Resio and Perrie (1991). Results from those tests were virtually identical to the FBM results and lend considerable confidence to the above statements regarding the inability of the WAMDIG source terms to reproduce the JONSWAP results. Many simple modifications to the WAMDIG source terms were attempted in an effort to improve the agreement with the JONSWAP relationships. However, these strictly empirical attempts did not seem to work particularly well and required massive amounts of computer time for each experimental run.

Alternative Source Term Formulation

From the above results and discussion, it is evident that some theoretical guidance is necessary to obtain source functions that are capable of reproducing the JONSWAP relationships. Since wave-wave interactions are conservative, all energy entering a wave field must be derived directly or indirectly from atmospheric input. From fundamental analyses of scaling functions of fluxes from high to low frequency and from low to high frequency, it can be

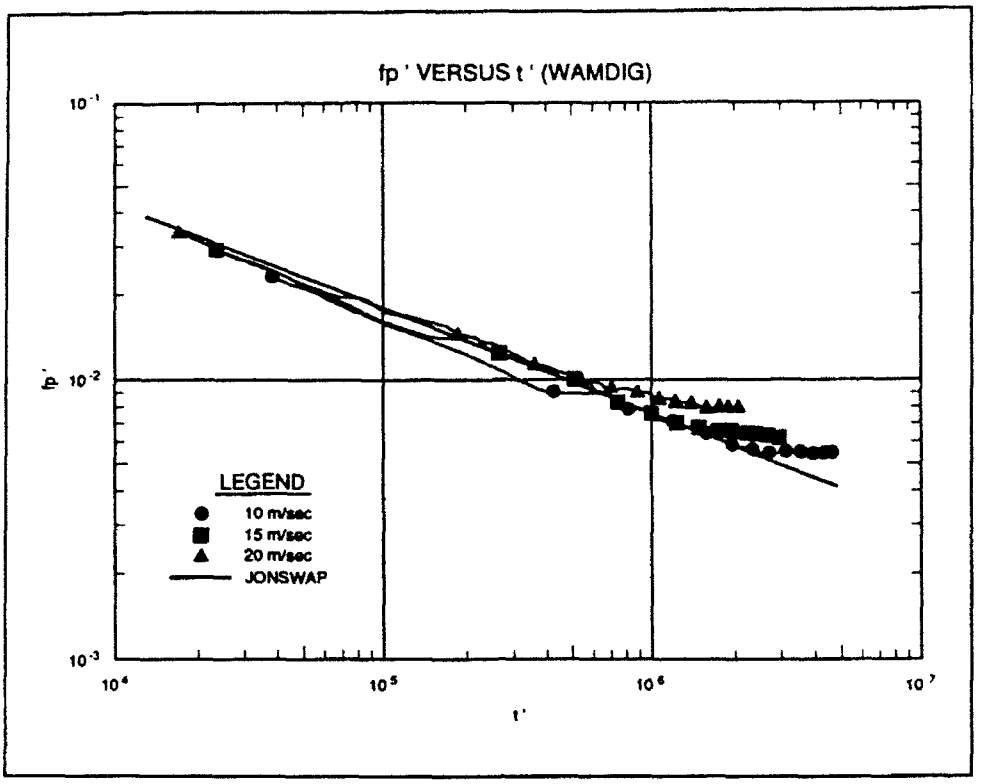

Figure 11. Comparison of FBM nondimensional peak frequency growth rate with time (using WAMDIG (1988) source terms) to JONSWAP results

shown that at least one "null-point frequency" f_n must exist within a spectrum such that fluxes from high to low frequencies exactly balance fluxes from low to high frequencies (for all nonlinear source terms with at least three lobes). An important consequence of the existence of this frequency is that there can be no net transfer of energy between regions on either side of it. Recognizing that the primary contribution to wave growth must come from inputs to frequencies less than f_n, the net gain of wave energy in a spectrum can be estimated from the relationship

$$\frac{\partial E_0}{\partial t} = \int_0^{f_n 2\pi} \int_0 S_{in}(f,\theta) + S_{ds}(f,\theta)\, df d\theta \tag{13}$$

The advantage of this form for net wave growth is that it removes the need for computer-intensive calculations of S_{nl}. Given a parametric relationship between f_n and f_p and an approximate spectral form for the spectral peak, Equation 13 can be used to estimate wave growth with little loss of accuracy. From numerical experiments with the full Boltzmann integral, it was determined that f_n is approximately equal to 1.5 f_p for spectra typical of the JONSWAP experiment (peakedness values in the range of 2.5 to 3.5). This

relationship provides closure for an accurate parametric approach to evaluating various source terms without having to evaluate S_{nl}.

It has been shown (Resio and Perrie 1989) that the JONSWAP relationship for wave growth along a fetch is consistent with a constant rate of momentum being transferred from the atmosphere. In order for a constant momentum flux (M_0) to exist,

$$\frac{\partial M_0}{\partial t} \approx \frac{1}{c_p}\frac{\partial E_0}{\partial t} = \text{constant} \tag{14}$$

where c_p is the phase velocity of the spectral peak frequency. Combining Equations 13 and 14, S_{in} for a self-similar growth of the JONSWAP type should have the form

$$S_{in} = bf\frac{\rho_a}{\rho_w}\left[\frac{u_*}{c_p}\right]^{4/3} H(u/c)E(f,\theta) \tag{15}$$

where $H(u/c)$ is a Heaviside function. This form is similar to that suggested by Resio and Perrie (1989). It is also close to the Snyder et al. (1981) representation of S_{in}, so it is not contradictory to observational evidence. It should be noted that this preserves a u_*-scaling relationship for momentum input during wave growth and a u-scaling for fully developed conditions.

Following arguments similar to those used for S_{in}, S_{ds} must have constraints on it that will allow Equation 14 to be met in order to achieve consistency with the JONSWAP results. Uncomplicating the WAMDIG form and allowing it to have a wind speed dependence as suggested by Banner and Phillips (1974),

$$S_{ds} = \lambda f\left[\frac{u_*}{c_p}\right]^{4/3} E(f,\theta) \tag{16}$$

This representation of S_{ds} is consistent with observational evidence and allows a self-similar form for wave growth.

Equations 15 and 16 for S_{in} and S_{ds}, respectively, provide an alternate set of source terms that can be used in conjunction with the full integral form for S_{nl} in FBM. Figures 12-15 show the computed nondimensional duration and fetch relationships for tests with 10-, 15-, and 20-m/sec wind speeds. These results are much closer to the JONSWAP relationships and are recommended for use in any operational version of FBM. One point worth noting in Figures 12-15 is that the asymptotes for the different wind speeds tested do not approach the same values. The reason for this is that the fully developed sea is based on a wind speed scaling, whereas friction velocity is used to scale E'. Thus, the tendency toward different asymptotic values is as expected.

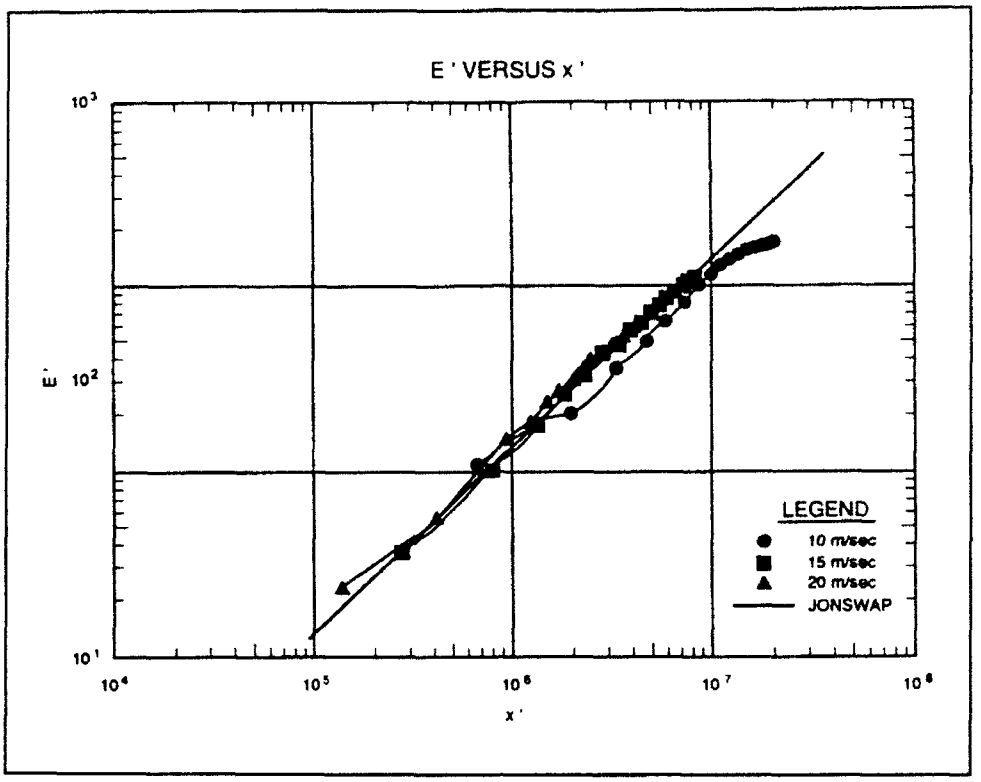

Figure 12. Comparison of FBM nondimensional energy growth rate with fetch (using new source terms) to JONSWAP results

Another small discrepency in the behavior of FBM is evident in a small offset in both wave energy and peak frequency as they move from a spectral peak in region III to a spectral peak in region II. It is very difficult to merge the two different solution methods (parametric versus detailed balance) into a smooth transition through this interface. However, once the spectrum reaches the discrete spectral range (presumably where one's primary interest lies), solutions for all wind speeds become very self-similar.

As a final point in this chapter, it should be noted that the location of f_n in the numerical tests was found to be highly dependent on the densities in the parametric spectral region (region III). This helps to explain the marked dependence of wave growth on the treatment of the high-frequency tail of the spectrum. Since there is no definitive concept of the characteristic behavior of the spectrum in this region, the following assumptions have been made for the equilibrium range densities in this region. Very importantly, for frequencies from up to 2.5 times the spectral peak frequency, energies are allowed to equilibrate to levels dictated by the "detailed balance" of all source terms. If this region extends into region III, an f^{-4} form as described in Resio and Perrie (1989) was used to constrain the energies. For frequencies above 2.5 times the spectral peak frequency (in both regions II and III), the equilibrium range is

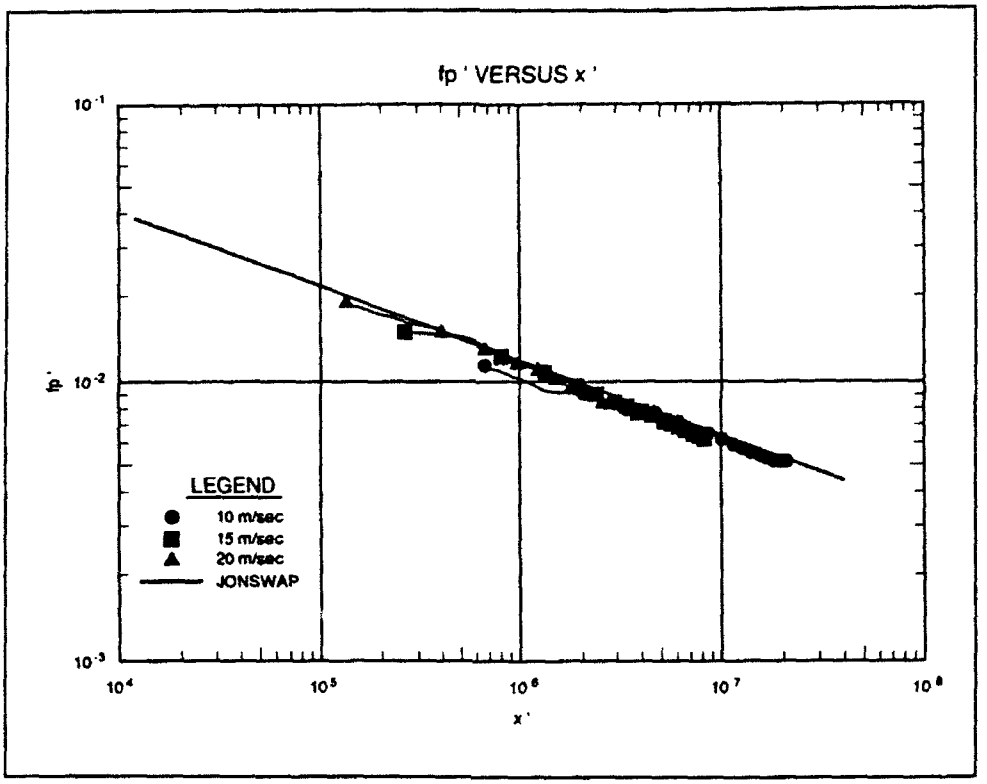

Figure 13. Comparison of FBM nondimensional peak frequency growth rate with fetch (using new source terms) to JONSWAP results

allowed to go to an f^{-5} form with equilibrium densities consistent with the JONSWAP relationship. This transition from an f^{-4} to an f^{-5} characteristic form is consistent with the findings of Kitaigorodskii (1983) and Hansen et al. (1990), except that the transition point in these other studies was somewhat higher (approximately $3f_p$) than in FBM.

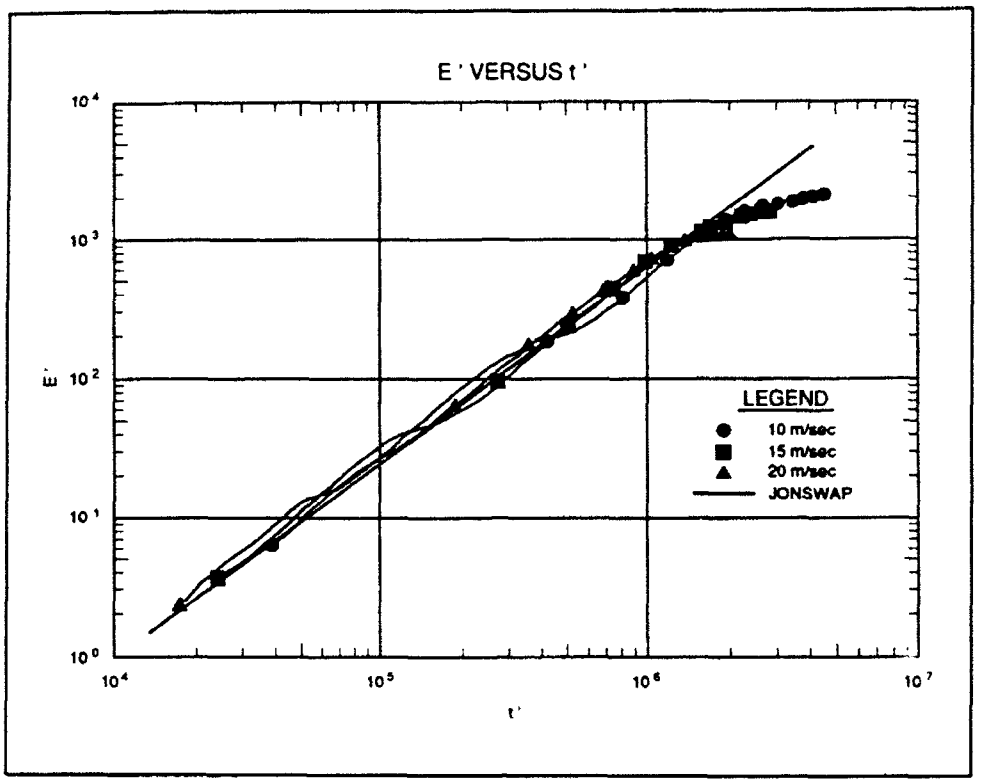

Figure 14. Comparison of FBM nondimensional energy growth rate with time (using new source terms) to JONSWAP

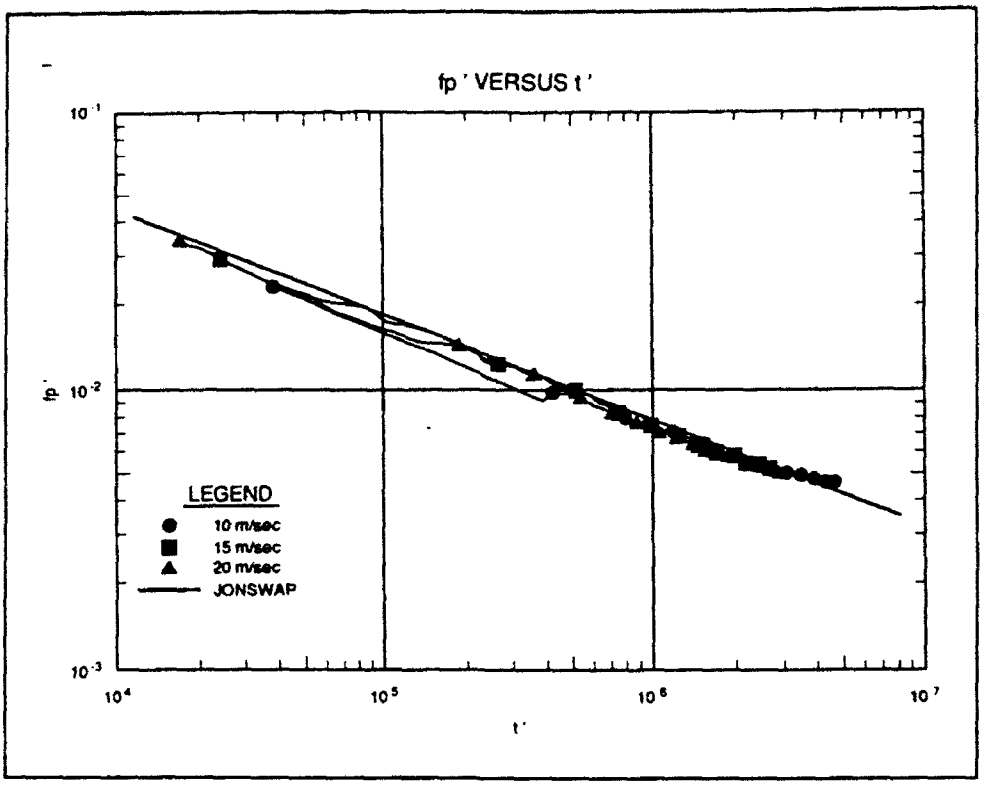

Figure 15. Comparison of FBM nondimensional peak frequency growth rate with time (using new source terms) to JONSWAP results

5 Additional Testing

Introduction

In order to demonstrate the basic functionality of a wave model, it is desirable to subject that model to as wide a range of tests as possible. Possibly the most important of these tests, model performance in reproducing the nondimensional JONSWAP relationships, was covered in the last section. However, certain other tests can provide important information regarding the behavior of FBM in future applications and can help distinguish important differences in the behavior of FBM relative to second-generation models and previous third-generation models. Three sets of comparisons will be made here:

a. Model performance in turning-wind situations.

b. Spectral distributions of energy produced by FBM:

(1) With respect to frequency.

(2) With respect to angle.

c. Prediction of swell evolution.

Model Performance in Turning-Wind Situations

To test FBM under turning wind situations, FBM was again run with a very large grid size (100,000 km) with only a single grid point in the water, as was done in the duration tests conducted in Chapter 4. The wind speed was set to 20 m/sec at 90 deg[1] (blowing toward the north) and allowed to remain constant for 10 hr. At the end of 10 hr, the wind speed remained constant and the wind direction was shifted. Two test runs were completed using the new source terms described in the previous section. In the first run, the wind was shifted to 45 deg (a 45-deg shift) and in the second the wind direction was shifted to 0 deg (a 90-deg shift). Figures 16 and 17 show the evolution of the

[1] To convert degrees (angle) to radians, multiply times a factor of 0.01745329.

mean wave angle following the 45-deg shift and 90-deg shift, respectively. Figure 18 shows the behavior of the mean angle as a function frequency following the 45-deg shift. In this figure the mean angle for a given frequency is defined as

$$\mu(f) = \tan^{-1}[\sum_y / \sum_x]$$

where

$$\sum_x = \int_0^{2\pi} E(f,\theta)\cos\theta \; d\theta \tag{17}$$

and

$$\sum_y = \int_0^{2\pi} E(f,\theta)\sin\theta \; d\theta$$

These results are in agreement with observations of Hasselmann, Dunckel, and Ewing (1980) and Gunther, Rosenthal, and Dunckel (1981) and show the same general trends as obtained in the numerical experiments of Young, Hasselmann, and Hasselmann (1987).

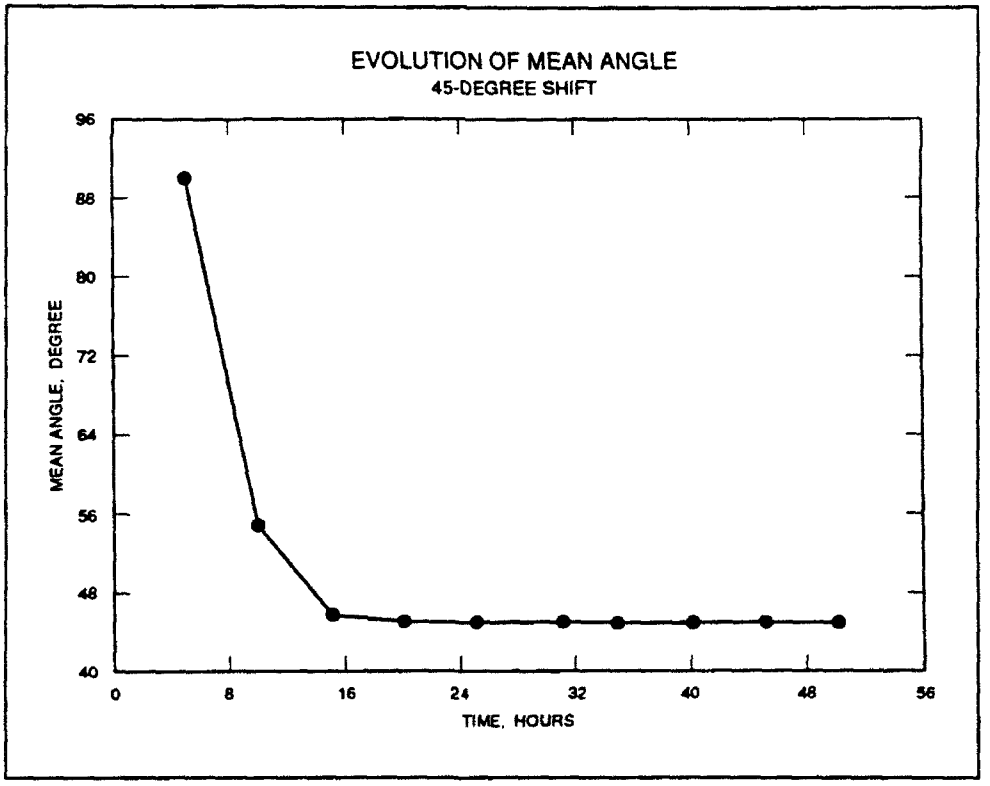

Figure 16. Evolution of mean wave angle following a 45-deg wind shift at hour 5

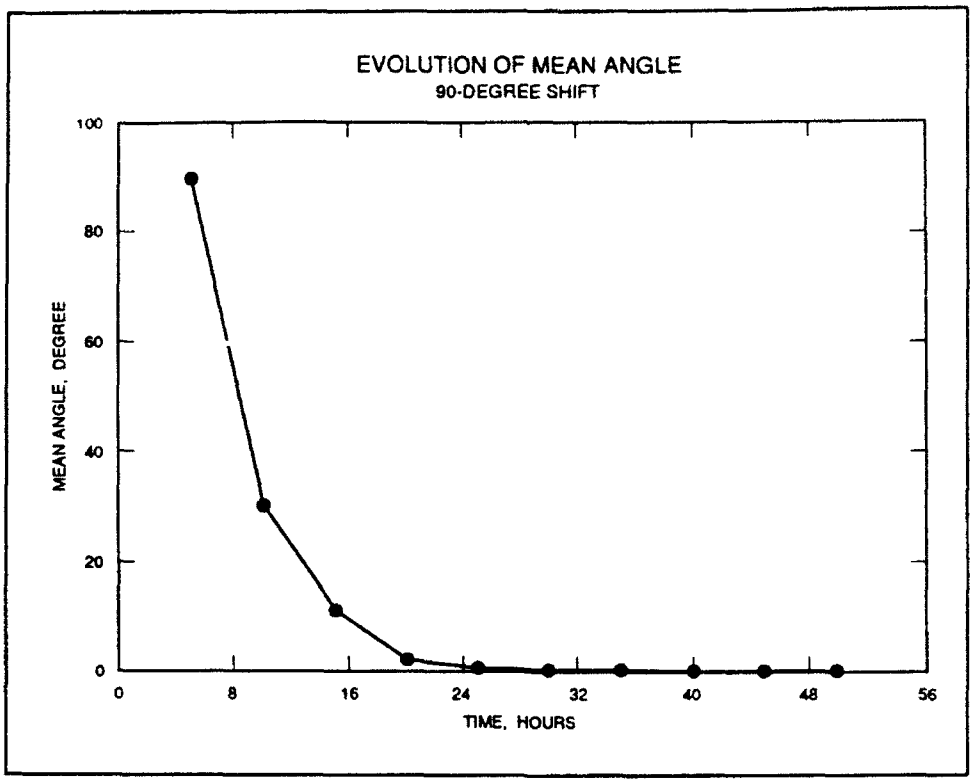

Figure 17. Evolution of mean wave angle following a 90-deg wind shift at hour 5

Spectral Distributions of Energy Produced by FBM

With respect to frequency

Figure 19 shows frequency specta at 10-hr intervals from a 20-m/sec duration test up to 50 hr. Figure 20 shows the same spectra normalized by multiplying them by f^4, i.e.,

$$E'(f) = E(f)f^4$$

It is evident from these figures that FBM produces smooth, regular spectral shapes that have similar characteristics to those observed in nature. At the spectral peak, the energy is about twice that of the equilibrium range energies, similar to the f^4- normalized spectra of Donelan, Hamilton, and Hui (1985). In the region from about 1.5 f_p to 2.5 f_p, the spectrum follows an approximate f^{-4} spectral form, consistent with many recent observations and theoretical analyses (Forrestall 1981; Donelan, Hamilton, and Hui 1985; Kahma 1981; Kitaigorodskii 1983). Above 2.5 f_p the spectrum shifts to an f^{-5} form, as stipulated in Chapter 4.

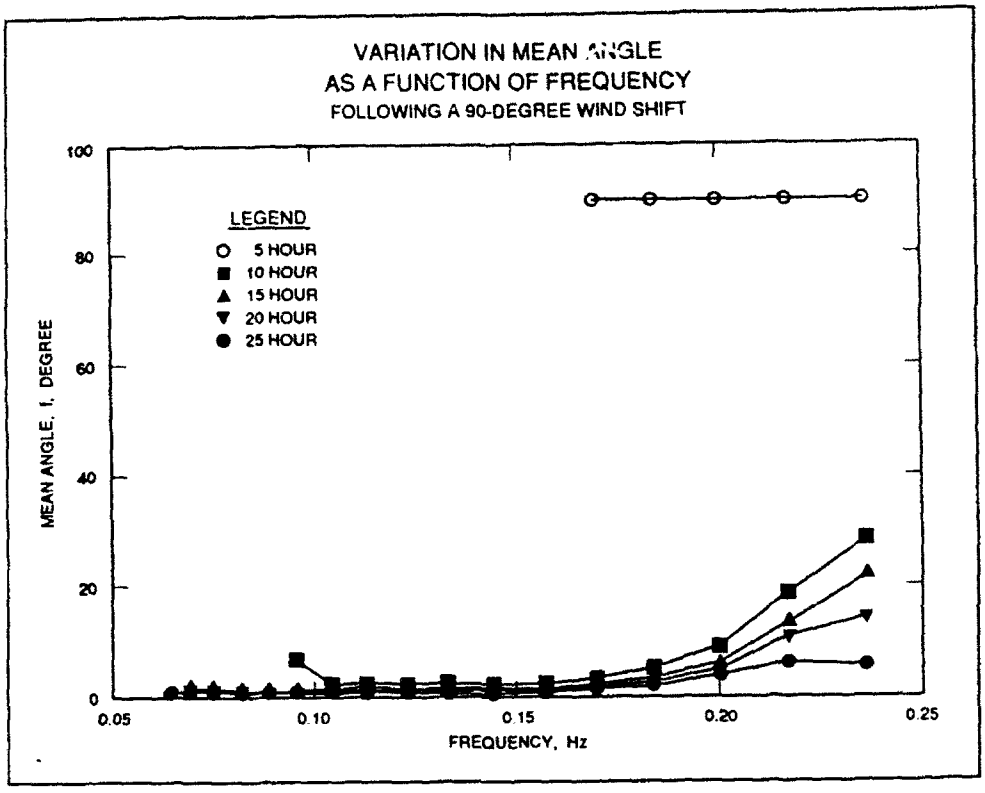

Figure 18. Variation in mean angle as a function of frequency following a 90-deg wind shift at hour 5

With respect to angle

Figure 21 shows the distribution of energy for frequencies of 0.8, 1.0, 2.0, and 3.0 f_p after 20 hr with a 20-m/sec wind speed and constant direction. As can be seen there, the spectral width is narrowest near the spectral peak and widest at high frequencies, consistent with observations of Mitsuyasu et al. (1975) and Hasselmann, Dunckel, and Ewing (1980). If an angular distribution function is defined as

$$E(f,\theta) = E(f)\,A(f,\theta)$$

where

$$\int_0^{2\pi} A(f,\theta)\,d\theta = 1 \tag{18}$$

and

$$A(f,\theta) = \pi^{-1}\sum_{n=1}^{\infty} a_n \cos n\theta + b_n \sin n\theta$$

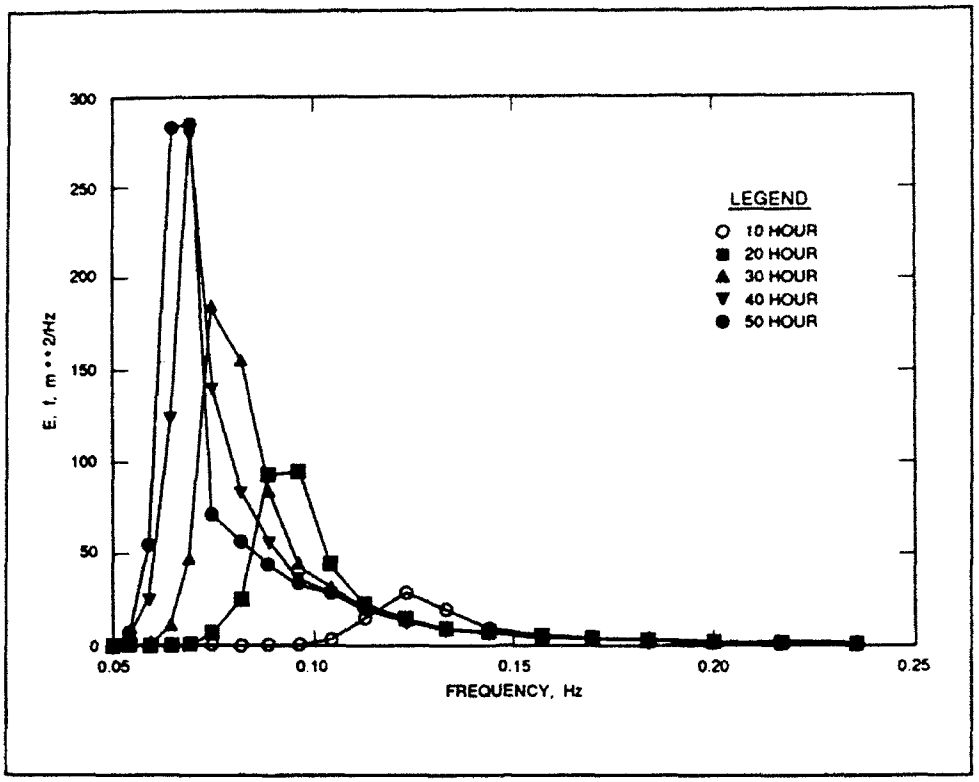

Figure 19. Spectral shapes for 10-hr intervals generated by FBM with a constant 20-m/sec wind speed

based on the Longuet-Higgins, Cartwright, and Smith (1963) analysis, then the angular energy distribution can be parameterized as

$$A(f,\theta) = \frac{1}{Z}(s)\cos^{2s}\left(\frac{\theta-\theta_0}{2}\right)$$

where (19)

$$Z(f) = \left|\int_0^{2\pi}\cos^{2s}\left(\frac{\theta-\theta_0}{2}\right)\,d\theta\right|^{-1}$$

Hasselmann and Hasselmann (1981) summarize the empirical findings for the behavior of s as

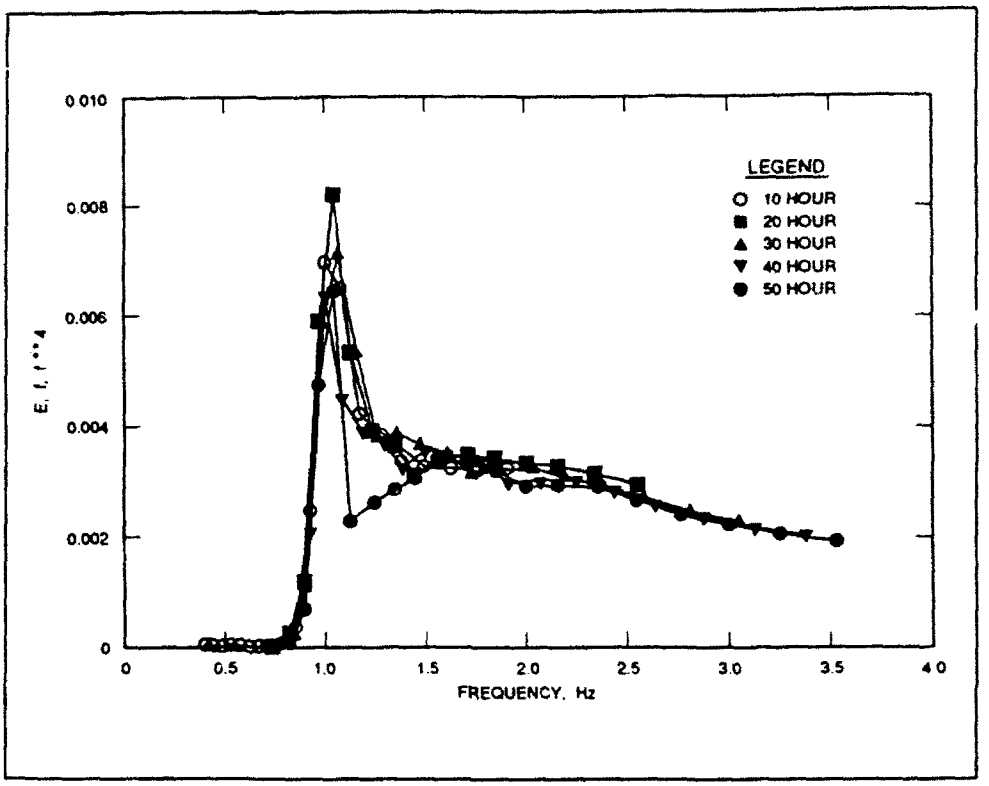

Figure 20. Normalized spectra [$E(f)f^4$] for same spectra shown in Figure 19

$$s = 9.77\,(f/f_p)^{\beta}$$

where

$$\beta = 4.06 \quad \text{for } f<f_p$$

$$\beta = -2.36 \quad \text{for } f \geq f_p \tag{20}$$

Figure 22 shows the variation of s as a function of f/f_p for the FBM spectra at hour 20 compared to this relationship. As can be seen there, there is a general agreement, but the wave spectra in FBM are not as broad (have higher s values) at high frequencies.

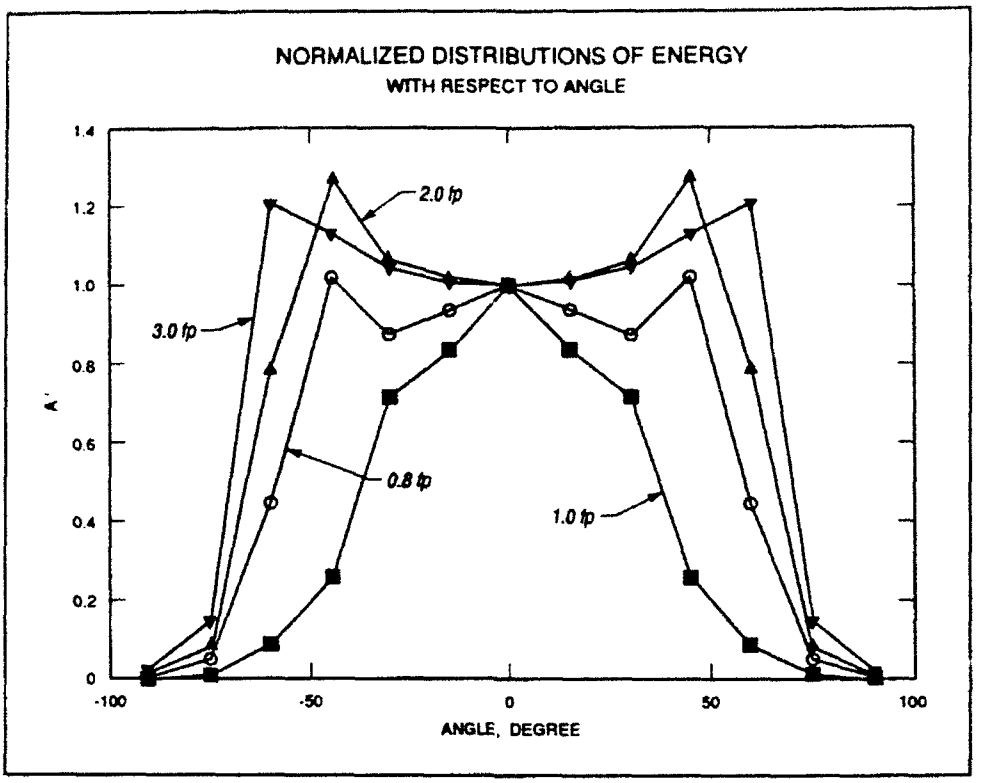

Figure 21. Angular distributions of energy normalized by the energy density of the central angle

Prediction of Swell Evolution

In second-generation wave models, swell decay is usually either treated as negligible and ignored, or is based on a simple scaling relationship. In the WAM model, the DIA (WAM's version of S_{nl}) is only calculated over frequencies in the local sea. S_{nl} for swell frequencies is assumed negligible. To test the capability of FBM to handle swell conditions, FBM was run with a 20-m/sec wind speed for 5 hr and wind speed was then lowered to 2 m/sec. Figure 23 shows the evolution of wave height and spectral peak wave period for this test. As can be seen there, the spectral peak continues to shift, and wave height decays after the wind is lowered. Models that neglect this effect are likely to underpredict wave periods for swell propagating over long distances.

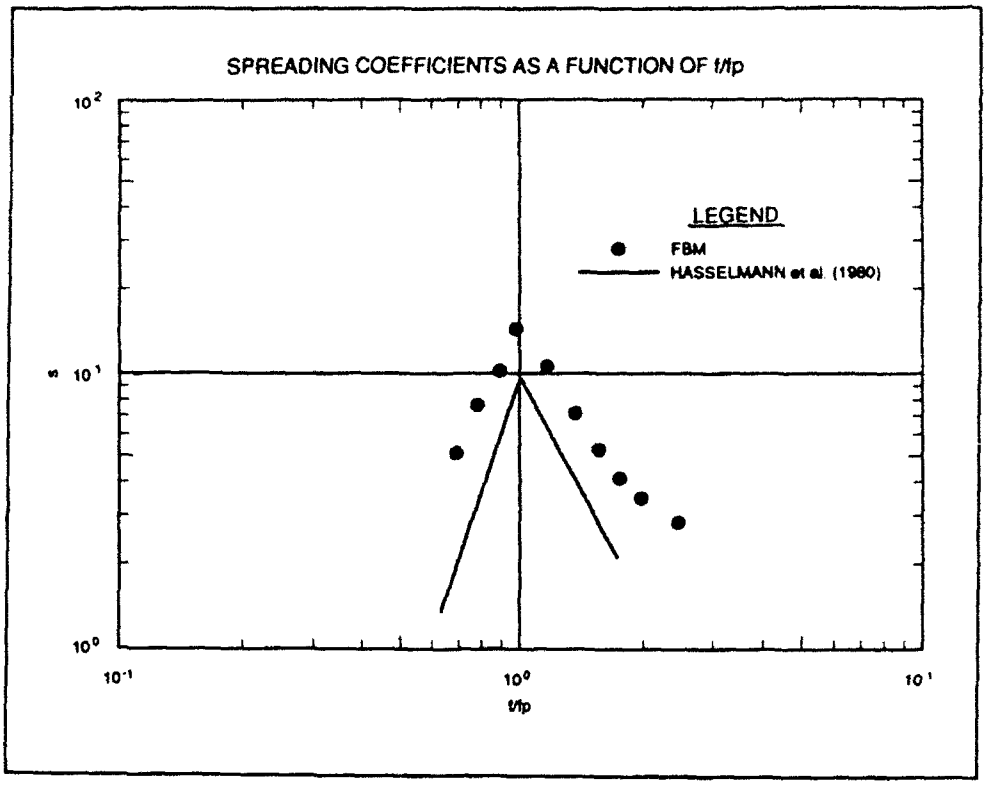

Figure 22. Comparison of values of "*s*" estimated for a spectrum from FBM to the Hasselmann, Dunckel, and Ewing (1980) relationship

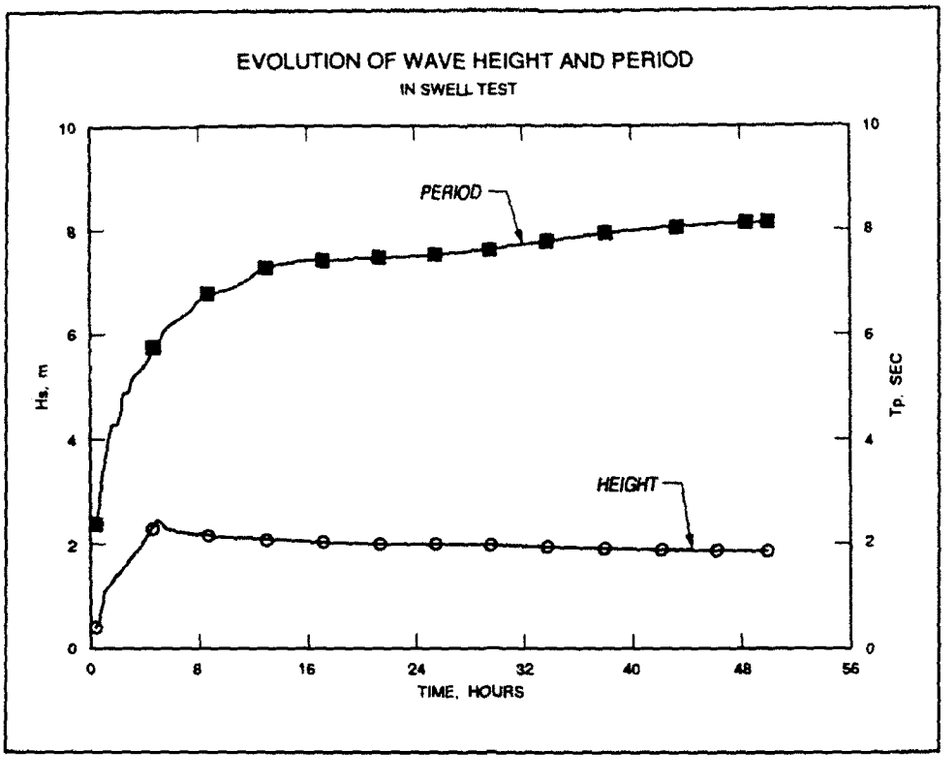

Figure 23. Evolution of wave height and period following a change in wind speed from 20 m/sec to 2 m/sec at hour 5

6 Summary and Conclusions

A full Boltzmann integration scheme has been implemented within a functioning discrete spectral wave model and preliminary testing has been completed. The following conclusions are drawn from the tests and analyses performed in this investigation:

a. Since third-generation models depend on a detailed balance among source terms, it is important that these source terms be specified accurately. In the present state of the art, information on all of the source terms does not appear to be sufficient to permit definitive estimates of all source terms in the detailed balance evaluation.

b. Older means of estimating S_{nl} are much less accurate than the full Boltzmann method used here. Even the DIA representation for S_{nl}, used in the only previous third-generation wave model (WAM), has been shown incapable of providing an accurate estimate of S_{nl}. The FBM should provide an improved method to investigate several important wave generation and decay situations. This could also markedly improve future second-generation wave models.

c. The WAMDIG source terms are inconsistent with observed wave-growth laws and equilibrium-range behavior from JONSWAP. These differences are very significant and cannot be removed by simple tuning.

d. New source terms postulated in this report provide a very good match to the JONSWAP wave growth rates and equilibrium-range behavior. These source terms are not inconsistent with previous theoretical and observational studies and are recommended for use in future applications and tests in FBM.

e. The performance of FBM in turning wind situations is consistent with previous theoretical and empirical studies.

f. Spectral shapes produced by FBM (using the new source terms postulated in this report) appear to provide a reasonable approximation to spectral shapes from observations. In particular, the spectral peakedness parameter is in the range of about 2.0 to 3.5 in the range of

actively growing seas and becomes much smaller as the fully developed condition is reached.

g. Swell decay in FBM is quite different from the WAM model and most second-generation models. In WAM, wave-wave interactions in swell are ignored and in second-generation models they are roughly parameterized. Tests in this study indicate that significant evolution of the spectral-peak frequency continues after the wind is abruptly lowered. This could explain much of the tendency of all present wave models to underpredict peak periods in swell. FBM results therefore could be a significant improvement in specifying waves for modeling coastal processes.

h. The current version of FBM should be regarded as a research tool. It is a very new model and, as such, will need to undergo considerable additional testing over several years before it could be considered as a viable option for an operational model.

References

Banner, M. L., and Phillips, O. M. (1974). "On the incipient breaking of small-scale waves," *J. Fluid Mech.* 65, 647-56.

Barnett, T. P. (1968). "On the generation, dissipation, and prediction of wind waves," *J. Geophys. Res.* 73, 647-56.

Barnett, T. P., and Sutherland, A. J. (1968). "A note on the overshoot effect in wind generated waves," *J. Geophys. Res.* 73, 6879-85.

Barnett, T. P., and Wilkerson, J. C. (1967). "On the generation of ocean waves as inferred from airborne radar measurements of fetch-limited spectra," *J. Mar. Res.* 25, 292-321.

Bretschneider, C. L. (1952). "Revised wave forecasting relationships." *Proc. 2nd International Conf. on Coastal Engr., American Society of Civil Engineers*, Berkeley, CA, 1-5.

Bunting, D. C. (1970). "Evaluating forecasts of ocean-wave spectra," *J. Geophys. Res.* 75, 4131-43.

Cardone, V. J., Pierson, W. J., and Ward, E. G. (1976). "Hindcasting the directional spectrum of hurricane generated waves," *J. of Petroleum Technology* 28.

Donelan, M. A., Hamilton, J., and Hui, W. H. (1985). "Directional spectra of wind-generated waves." *Phil. Trans. R. Soc. Lond.* Ser. A (315), 509-62.

Ewing, J. A. (1971). "A numerical wave prediction method for the North Atlantic Ocean," *Deutsche Hydrographische Zeitshrift* 24, 241-61.

Forristall, G. Z. (1981). "Measurements of saturated range in ocean wave spectra," *J. Geophys. Res.* 86, 8075-89.

Gelci, R., Cazalé, H., and Vassal, J. (1957). "Prévision de la houle -La méthod des densités spectroangulaires," Bull. Inform. *Comité Central Oceanogr. D'Etude Côtes* 9, 416-35.

Gunther, H., Rosenthal, W., and Dunckel, M. (1981). "The response of surface gravity waves to changing wind direction," *J. Phys. Oceanogr.* 11, 718-28.

Hansen, C., Katsaros, K. B., Kitaigorodskii, S. A., and Larsen, S. E. (1990). "The dissipation range of wind-wave spectra observed on a lake," *J. Phys. Oceanogr.* 20, 1264-77.

Hasselmann, D. E., Dunckel, M., and Ewing, J. A. (1980). "Directional wave spectra observed during JONSWAP 1973," *J. Phys. Oceanogr.* 10, 1264-80.

Hasselmann, K. (1962). "On the non-linear energy transfer in a gravity-wave spectrum - Part 1," *J. Fluid Mech.* 12, 481-500.

_____. (1963a). "On the non-linear energy transfer in a gravity-wave spectrum - Part 2," *J. Fluid Mech.* 15, 273-81.

_____. (1963b). "On the non-linear energy transfer in a gravity-wave spectrum - Part 3," *J. Fluid Mech.* 15, 385-98.

_____. (1974). "On the spectral dissipation of ocean waves due to white capping," *Bound.-Layer Meteor.* 6, 107-27.

Hasselmann, K., Barnett, T. P., Bouws, E., Carlson, H., Cartwright, D. E., Enke, K., Ewing, J. A., Gienapp, H., Hasselmann, D. E., Kruweman, P., Meerburg, A., Muller, P, Olbers, K. J., Richter, K., Sell, W., and Welden, W. H. (1973). "Measurements of wind-wave growth and swell decay during the Joint North Sea Wave Project (JONSWAP)," *Deutsche Hydrograph. Zeit., Erganzung-sheft Reihe A (8^{o})*, 12.

Hasselmann, K., Ross, D. B., Muller, P., and Sell, W. (1976). "A parametric wave prediction model," *J. Phys. Oceanogr.* 6, 200-28.

Hasselmann, S., and Hasselmann, K. (1981). "A symmetrical method of computing the nonlinear transfer in a gravity-wave spectrum," *Hamburger Geophys. Einzelshr.* A52.

_____. (1985). "Computation and parameterization of the nonlinear energy transfer in a gravity wave spectrum - Part 1," *J. Phys. Oceanogr.* 15, 1369-77.

Hasselmann, S., Hasselmann, K., Allender, J. H., and Barnett, T. P. (1985a). "Computation and parameterization of the nonlinear energy transfer in a gravity wave spectrum - Part 2," *J. Phys. Oceanogr.* 15, 1378-91.

Hasselmann, S., Hasselmann, K., Komen, G. K., Janssen, P., Ewing, J. A., and Cardone, V. J. (1985b). "The WAM model - A third generation ocean wave prediction model," *J. Phys. Oceanogr.* 18, 1775-1810.

Hubertz, J. M. (1992). "User's guide to the wave information studies (WIS) wave model, version 2.0," WIS Rep. No. 27, U.S. Army Engineer Waterways Experiment Station, Vicksburg, MS.

Inoue, T. (1967). "On the growth of the spectrum of a wind generated sea according to a modified Miles-Phillips mechanism and its application to wave forecasting," New York Univ. Geophys. Sci. Lab. Rep. 67-5.

Kahma, K. K. (1981). "A study of the growth of the wave spectrum with fetch," *J. Phys. Oceanogr.* 11, 1503-15.

Kitaigorodskii, S.A. (1961). "Application of the theory of similarity to the analysis of wind-generated wave motion as a stochastic process," Bull. Acad. Sci. USSR Ser. Geophys. 1, (1), 33-62.

_____. (1983). "On the theory of the equilibrium range on the spectrum of wind-generated gravity waves," *J. Phys. Oceanogr.* 13, 816-27.

Komen, G. J., Hasselmann, S., and Hasselmann, K. (1984). "On the existence of a fully developed windsea spectrum," *J. Phys. Oceanogr.* 14, 1271-85.

Longuet-Higgins, M. S., Cartwright, D. E., and Smith, N. D. (1963). "Observations of the directional spectrum of sea waves using the motions of a floating buoy," *Ocean Wave Spectra*, Prentice-Hall, 111-36.

Miles, J. W. (1957). "On the generation of surface waves by turbulent shear flows," *J. Fluid Mech.* 7, 469-78.

Mitsuyasu, H. (1968a). "A note on the nonlinear energy transfer in the spectrum of wind-generated waves," Rep. Res. Inst. for Appl. Mech., Kyushu Univ., Fukuoka, Japan, 16, 251-64.

_____. (1968b). "On the growth of wind-generated waves (1)," Rep. Res. Inst. for Appl. Mech, Kyushu Univ., Fukuoka, Japan, 16, 459-82.

Mitsuyasu, H., Tasai, F., Suhara, T., Mizuno, S., Ohkuso, N., Honda, T., and Rikiishi, K. (1975). "Observations of the directional spectra of ocean waves using a cloverleaf buoy," *J. Phys. Oceanogr.* 5, 750-60.

Perrie, W. and Resio, D. T. (1993). "A numerical study of nonlinear fluxes in a wave spectrum: Part 2 - Equilibrium range constraints," submitted to *J. Phys. Oceanogr.*

Phillips, O. M. (1957). "On the generation of waves by turbulent wind," *J. Fluid Mech.* 2, 417-45.

_____. (1958). "The equilibrium range in the spectrum of wind-generated waves," *J. Fluid Mech.* 4, 426-34.

Pierson, W. J., and Moskowitz, L. (1964). "A proposed spectral form for fully developed wind seas based on the similarity theory of S.A. Kitaigorodskii," *J. Geophys. Res.* 9, 5181-90.

Pierson, W. J., Neumann, G., and James, R. W. (1955). "Observing and forecasting ocean waves by means of wave spectra and statistics," H. O. Pub. No. 603, U.S. Navy Hydrographical Office, Washington, DC.

Resio, D. T. (1981). "The estimation of wind-wave generation in a discrete spectral model," *J. Geophys. Res.* 11, 510-25.

Resio, D. T., and Perrie, W. (1989). "Implications of an f^{-4} equilibrium range for wind-generated waves," *J. Phys. Oceanogr.* 19, 193-204.

_____. (1991). "A numerical study of nonlinear energy fluxes due to wave-wave interactions - Part 1," *J. Fluid Mech.* 223, 603-29.

Resio, D. T., and Vincent, C. L. (1982). "Comparison of various wave prediction methods," *J. Petrol. Tech.*

Snyder, R. L., Dobson, F. W., Elliott, J. A., and Long, R. B. (1981). "Array measurements of atmospheric pressure fluctuations above surface gravity waves," *J. Fluid Mech.* 102, 1-59.

Sverdrup, H. U., and Munk, W. H. (1947). "Wind, sea and swell - theory of relations for forecasting," H. O. Pub. No. 601, U.S. Navy Hydrographical Office, Washington, DC.

Toba, Y. (1978). "Stochastic form of the growth of wind waves in a single-parameter representation with physical implications," *J. Phys. Oceanogr.* 8, 494-507.

Toba, Y., Okada, K., and Jones, I. S. F. (1988). "The response of wind-wave spectra to changing winds. Part I: Increasing winds," *J. Phys. Oceanogr.* 18, 1231-40.

Tracy, B. A., and Resio, D. T. (1978). "Theory and calculation of the nonlinear energy transfer between sea waves in deep water," Wave Information Study Rep. No. 11, U.S. Army Engineer Waterways Experiment Station, Vicksburg, MS.

_____. (1982). "Theory and calculation of the nonlinear energy transfer between sea waves in deep water," WIS Rep. No. 11, U.S. Army Engineer Waterways Experiment Station, Vicksburg, MS.

Vincent, C. L., and Resio, D. T. (1977). "An Eigenfunction parameterization of a time series of wave spectra," *Coastal Engr.* 1, 185-205.

WAMDIG. (1988). "The WAM model - a third generation ocean wave prediction model," *J. Phys. Oceanogr.* 18, 1775-1810.

Webb, D. J. (1978). "Nonlinear transfer between sea waves," *Deep-Sea Res.* 25, 279-98.

Young, I. R., Hasselmann, S., and Hasselmann, K. (1987). "Computations of the response of a wave spectrum to a sudden change in wind direction," *J. Phys. Oceanogr.* 17, 1317-38.

REPORT DOCUMENTATION PAGE

Form Approved
OMB No. 0704-0188

1. AGENCY USE ONLY (Leave blank)	2. REPORT DATE	3. REPORT TYPE AND DATES COVERED
	August 1993	Final report

4. TITLE AND SUBTITLE

Full Boltzmann Discrete Spectral Wave Model, Implementation and Nondimensional Tests

5. FUNDING NUMBERS

6. AUTHOR(S)

Donald T. Resio

7. PERFORMING ORGANIZATION NAME(S) AND ADDRESS(ES)

Department of Oceanography, Ocean Engineering, and Environmental Science
Florida Institute of Technology
Melbourne, FL 32901

8. PERFORMING ORGANIZATION REPORT NUMBER

9. SPONSORING / MONITORING AGENCY NAME(S) AND ADDRESS(ES)

Headquarters, U.S. Army Corps of Engineers
Washington, DC 20314-1000;
USAE Waterways Experiment Station, Coastal Engineering Research Center, 3909 Halls Ferry Road, Vicksburg, MS 39180-6199

10. SPONSORING / MONITORING AGENCY REPORT NUMBER

Contract Report
CERC-93-1

11. SUPPLEMENTARY NOTES

Available from National Technical Information Service, 5285 Port Royal Road, Springfield, VA 22161

12a. DISTRIBUTION / AVAILABILITY STATEMENT

Approved for public release; distribution is unlimited.

12b. DISTRIBUTION CODE

13. ABSTRACT *(Maximum 200 words)*

A full Boltzmann integration scheme is implemented within a functioning discrete spectral wave model. Preliminary testing (academic) is presented and compared to alternate solution methods. It is found that third-generation models depend on a detailed balance among source terms, and it is important that these source terms be specified accurately. In the present state of the art, information on all of the source terms does not appear to be sufficient to permit definitive estimates of all source terms in the detailed balance evaluations. Older means of estimating the nonlinear wave-wave interaction (S_{nl}) are much less accurate than the full Boltzmann method. Even the Discrete Interaction Approximation (WAMDIG 1988) representation for S_{nl}, used in the only documented third-generation wave model (WAM), is shown incapable of providing an accurate estimate of S_{nl}. The full Boltzmann model should provide an improved method to investigate several important wave generation and decay situations. The WAM source terms are inconsistent with observed wave-growth laws and equilibrium-range behavior from the Joint North Sea Wave Project (Hasselmann et al. 1973). New source terms postulated in this report provide a very good match to the JONSWAP wave growth rates and equilibrium-range behavior. The present version of the full Boltzmann model should be regarded as a research tool. It is a very new model and, as such, will need to undergo considerable additional testing over several years before it could be considered as a viable option for an operational model.

14. SUBJECT TERMS

Numerical model
Water waves
Wave spectra

15. NUMBER OF PAGES

51

16. PRICE CODE

17. SECURITY CLASSIFICATION OF REPORT	18. SECURITY CLASSIFICATION OF THIS PAGE	19. SECURITY CLASSIFICATION OF ABSTRACT	20. LIMITATION OF ABSTRACT
UNCLASSIFIED	UNCLASSIFIED		